

Forschungszentrum Karlsruhe

in der Helmholtz-Gemeinschaft

FZKA Technical Report

Investigations of COBRA-EN and COBRA-TF for
core and assembly simulations and coupling of
COBRA-TF and KARBUS

Björn BECKER

Ecole Nationale Supérieure de Physique de Grenoble
ENSPG



Forschungszentrum Karlsruhe GmbH, Karlsruhe

2005

Rapport de stage 2A GEN

BECKER Björn

Mail: bjorn.becker@gmx.de

Mobil: 06 88 15 02 80

ABSTRACT:

The following report presents core and assembly simulations of the active part of the pressurized water reactor GKN2 core (type KONVOI). The simulations were made with the thermo hydraulic subchannel codes COBRA-EN and COBRA-TF. The analyzed situation is a normal function of the PWR. The core is completely filled with water and a steady state situation is reached. The results of both codes are compared and several problems revealed.

A second focus of this report is set on a coupling method/interaction of COBRA-TF and the neutronic code KARBUS, which was realized. A coupled simulation was performed and a changing of the power rating was observed.

Keywords: COBRA-EN, COBRA-TF, subchannel analysis, KONVOI, GKN2, coupling, KARBUS

RESUME:

Ce rapport présente des simulations du cœur et d'un assemblage de la partie active du réacteur à eau pressurisée GKN2 (type KONVOI). Les simulations ont été faites avec les logiciels thermohydrauliques COBRA-EN et COBRA-TF. La situation analysée est un fonctionnement normal du REP. Cela signifie que le cœur est complètement rempli d'eau et qu'une situation stable est atteinte. Les résultats des simulations sont été comparés et de multiples problèmes ont été révélés. Ensuite ce rapport met l'accent sur une méthode d'un couplage de COBRA-TF et du code neutronique KARBUS, qui était réalisé. Une simulation couplée a été effectuée et on a observé un changement de la puissance des barres de combustible.

Mots de clé : COBRA-EN, COBRA-TF, subchannel analysis, KONVOI, GKN 2, couplage, KARBUS

ZUSAMMENFASSUNG:

Der folgende Bericht präsentiert Kern- und Brennelementsimulationen vom GKN2 Reaktorkern (Type KONVOI). Die Simulationen wurden mit den thermohydraulischen Subchannel Codes COBRA-EN und COBRA-TF durchgeführt. Der Kern ist komplett mit Wasser gefüllt und ein stationärer Zustand wird erreicht. Die Ergebnisse beider Codes werden verglichen und einige Probleme aufgedeckt.

Ein zweiter Schwerpunkt dieses Berichtes liegt auf einer Kopplungsmethode bzw. der Datenaustausch zwischen COBRA-TF und KARBUS, welche realisiert wurde. Eine gekoppelte Simulation wurde durchgeführt und eine Verschiebung der Leistung wurde beobachtet.

Keywords: COBRA-EN, COBRA-TF, subchannel analysis, KONVOI, coupling, KARBUS

ACKNOWLEDGMENTS:

In this place, I would like to thank several people who were important for my work and the time I spend at the IRS:

Dr. V. Sanchez Espinoza, he always found the time and the patience to answer all my questions and he received me so heartily. Working with him was very pleasant.

Dr. C.H.M. Broeders, working with him in the neutronic domain was very interesting and instructive.

J. Aberle, who welcomed me so friendly in his office and helped me with all my computer problems and all other colleagues, who always called me for lunch.

P. Oberle and L. Send, who had always time for having coffee and giving advices.

D. Weber, student colleague, who spend a lot time and patience trying to correct my horrible English.

TABLE OF CONTENT

CHAPTER 0 INTRODUCTION	1
Intention.....	1
CHAPTER 1 WORK ENVIRONMENT.....	3
1.1. FZK.....	3
1.2. IRS	4
Chapter 2 GENERAL DESCRIPTION OF THE SIMULATION OF GKN II	5
2.1. Description of the Reactor.....	5
2.2. Core.....	5
2.3. Assembly.....	6
Chapter 3 THEORETICAL BASIS.....	9
3.1. A thermo hydraulic subchannel analysis.....	9
3.2. A thermo hydraulic core analysis	9
3.3. Theoretical background of COBRA-EN	9
3.3.1. Flow Field Model.....	9
3.3.2. Heat Transfer Model	10
3.4. Theoretical background of COBRA-TF	11
3.4.1. Conservation equations	11
3.4.2. Heat Transfer Model	12
Chapter 4 SIMULATIONS	13
4.1. Simulations with COBRA-EN	13
4.1.1. Assembly analysis	13
4.1.2. Core analysis	18
4.1.3. Review on COBRA-EN	19
4.2. Simulation with COBRA-TF.....	20
4.2.1. Assembly analysis	20
4.2.2. Core analysis	25
4.2.3. Review on COBRA-TF.....	27
Chapter 5 COUPLING OF COBRA-TF AND KARBUS.....	29
5.1. Introduction	29
5.2. Coupling method	29
5.3. Post-processing of data	30
5.3.1. Post-processing of COBRA-TF output data	30
5.3.2. Post-processing of KARBUS output data	31
5.4. Transferring COBRA-TF from Windows to Linux.....	31
5.5. Results	31
Chapter 6 CONCLUSION	33
Chapter 7 PERSPECTIVES	33
Appendix A EQUATIONS	I
Appendix B CASMO DATA SHEET	V
Appendix C COBRA-EN FIGURES	VII
Appendix D HEADER FILE "RESPAR.H"	IX
Appendix E COBRA-TF INPUT FILE FOR AN ASSEMBLY ANALYSIS	XI
Appendix F COBRA-TF FILE: "SETUP.F"	XIX
Appendix G COUPLING RESULTS.....	XXI
Appendix H REFERENCES.....	XXIII

LIST OF FIGURES

Figure 2-1: 1/8 of core	5
Figure 2-2: CASMO-data for radial power.....	6
Figure 2-3: subchannel.....	6
Figure 2-4: fuel rod	6
Figure 2-5: 1/8 of an assembly.....	7
Figure 2-6: full assembly	7
Figure 2-7: relative rod power	7
Figure 3-1: fuel rod mesh	10
Figure 3-2: heat flux as function of superheat.....	11
Figure 4-1: CobraEN numbering	13
Figure 4-2: COBRA-EN assembly simulation without crossflow - coolant outlet temperature.....	14
Figure 4-3: COBRA-EN assembly simulation without crossflow - coolant outlet temperature.....	15
Figure 4-4: COBRA-EN assembly simulation without crossflow - coolant density.....	15
Figure 4-5: COBRA-EN assembly simulation without crossflow - clad temperature.....	16
Figure 4-6: COBRA-EN assembly simulation without crossflow - outer pellet temperature	16
Figure 4-7: COBRA-EN assembly simulation without crossflow - inner pellet temperature	16
Figure 4-8: COBRA-EN assembly simulation with crossflow - outlet coolant temperature.....	17
Figure 4-9: COBRA-EN assembly simulation - comparison open/closed channels.....	17
Figure 4-10: COBRA-EN core simulation (no radial dependency) - outlet coolant temperature	18
Figure 4-11: COBRA-EN core simulation (no radial dependency) - coolant temperature	18
Figure 4-12: COBRA-EN core simulation (radial dependency) - outlet coolant temperature	19
Figure 4-13: Heat added to Liquid for steady state verification.....	20
Figure 4-14: Rod surface temperature for steady state verification	20
Figure 4-15: COBRA-TF channel numbering.....	21
Figure 4-16: COBRA-TF gap numbering.....	21
Figure 4-18: COBRA-TF assembly simulation without crossflow - coolant outlet temperature	22
Figure 4-19: COBRA-TF assembly simulation without crossflow - coolant temperature	22
Figure 4-20: COBRA-TF assembly simulation without crossflow - coolant density	23
Figure 4-21: COBRA-TF assembly simulation without crossflow - pressure	23
Figure 4-22: COBRA-TF assembly simulation with crossflow - outlet coolant temperature	24
Figure 4-23: COBRA-TF assembly simulation - differences of outlet coolant temperature open/closed channels.....	24
Figure 4-24: Comparison of outlet coolant temperatures from COBRA-EN and COBRA-TF	25
Figure 4-25: Comparison coolant temperatures from COBRA-EN and COBRA-TF	25
Figure 4-26: COBRA-TF core simulation (no radial dependency) – coolant temperature	26
Figure 4-27: COBRA-TF core simulation (radial dependency) – outlet coolant temperature	26
Figure 4-28: comparison of COBRA-EN/TF core simulation (radial dependency) – outlet coolant temperature.....	27
Figure 5-1: Coupling scheme	30
Figure 5-2 Coupling - Axial power distribution [Ref. XI]	32
Figure B-1: Casmos radial power distribution	V
Figure C-1: COBRA-EN assembly simulation with crossflow - coolant temperature	VII
Figure C-2: COBRA-EN assembly simulation with crossflow - coolant density	VII
Figure C-3: COBRA-EN assembly simulation with crossflow - clad temperature	VIII
Figure C-4: COBRA-EN assembly simulation with crossflow - outer pellet temperature.....	VIII
Figure C-5: COBRA-EN assembly simulation with crossflow - inner pellet temperature.....	VIII
Figure G-1: Coupling - Water temperature [Ref. XI].....	XXI
Figure G-2: Coupling - fuel temperature [Ref. XI]	XXI
Figure G-3: Coupling - Water density [Ref. XI].....	XXII

Chapter 0

INTRODUCTION

Safety tests and analyses of nuclear reactor systems are indispensable for the safe use of nuclear energy. Therefore, researchers collaborate worldwide in order to improve the existing power plants and to advance the knowledge in nuclear engineering. In Germany, Karlsruhe with its research center FZK (*Forschungszentrum Karlsruhe*) is one of the main actors in this field. The Institute for Reactor Safety (*Institut für Reaktor Sicherheit - IRS*) is leading.

Numeric analyses are very common in nuclear engineering. They provide a basis for the improvement of working reactors and the development of new systems. They are essential for the study of accidents and their long-term consequences for the reactor. However, different codes lead to different results depending on the used physical models and the code precision. The predictions of the numeric codes are validated via experiments. These experiments may consist of a part of a reactor, for example a fuel rod or a rod bundle. In order to obtain high precision a numeric analysis has to take care of, among others, interaction between neutron and thermo hydraulic physics.

There are numerous reactor analysis tools. In general, these tools are categorized according to their analysis-domain and scale. A first approach is made by system tools (e.g. RELAP5 [Ref.i]) which simulate the whole reactor system (vessel and core, heat exchangers, tubes etc.). The next step is a core simulation which is made by either neutronic (e.g. PARCS [Ref.ii]) or thermo hydraulic codes (e.g. COBRA).

A neutronic code calculates primarily the radial and axial fuel rod power distribution. Nevertheless, it also can determine the "burn-up", the concentration of fission products. It demands input data like fluid density and rod temperature. The neutronic code domain is divided into probabilistic Monte-Carlo codes (e.g. MCNP, MCNPX [Ref.iii]) and deterministic codes (e.g. KARBUS).

A thermo hydraulic code treats the heat exchange of the fuel rod with the coolant. Void fraction (part of steam in liquid), turbulences and density are some of the outcomes. As input data, it demands not only the rod power but also the inlet temperature of the coolant, its velocity in axial direction and the vessel pressure.

These codes exist as stand-alone or already coupled versions (NORMA+COBRA-EN [Ref.iv]). The coupled codes exchange directly required input data.

A possible and intensive studied accident is a LOCA (Lost Of Coolant Accident) in a Pressurized Water Reactor (PWR). In this case, due to a tube break, the pressure in the vessel plunges down and boiling starts. The boiling surface starts to sink until the core is nearly completely filled with steam. This steam cannot evacuate as much heat as a liquid could because of its poorer heat coefficient. To avoid a core melt, cool liquid is abruptly entered in the core (quench) and the boiling surface rises.

Intention

The intention of this student research project was predominantly to investigate the prediction capability of both COBRA-EN and COBRA-TF by numerous of calculations of selected problems. In the main, other codes for thermo hydraulic calculations are used in the IRS institute. Therefore, little experience with these two codes could be transmitted. Problems should be encountered and documented. The results of both codes should be compared. The long-term ambition was to perform a coupling (loose connection) between COBRA-TF and the neutronic code KARBUS and to evaluate the consequences of this interaction.

Chapter 1

WORK ENVIRONMENT

1.1. FZK

The federal Republic of Germany and the State of Badenwürttemberg fund the research center in Karlsruhe, called *Forschungszentrum Karlsruhe GmbH in der Helmholtz-Gemeinschaft* (FZK).



Today, the FZK is one of the biggest independent research facilities in Germany. It is embedded and coordinated by the *Hermann von Helmholtz Association of National Research Centers*. Over all, 15 scientific-technical and biological-medical research centers of all parts of Germany have joined the community with the aim to gain knowledge that can help to preserve and improve human life. The Helmholtz Association has a budget of 2.2 billion euros and over 24 000 employees.

The FZK was founded 1956 and is located 12 km north of the city of Karlsruhe on an area of 2 km². The original task was the nuclear research and development. The FZK build for example the first German critical research reactor *FR2*, a heavy water cooled reactor (2% enriched UO₂) with a power of 44MW. However, since the eighties a broader spectrum of activities, than the nuclear engineering, is focused. The activities are now embedded in the program structure of the Helmholtz association, which concentrates on five research areas.

research area	FZK program
Structure of Matter	Structure of Matter
Earth and Environment	Sustainability and Technology Atmosphere and Climate
Health	Biomedical Research Regenerative Medicine
Energy	Nuclear Fusion Nuclear Safety Research Efficient Energy Conversion
Key Technologies	Nano-Microsystems Program Scientific Computing

Nevertheless, the FZK is still the first competence for nuclear engineering. The research center tries to maintain nuclear engineering knowledge in times where young scientific-technical staff for this area is hard to find.

The FZK has about 3800 employees. 1420 scientists, 60 professors and 185 pre-doctoral students work in 22 different institutes. The FZK has a strong cooperation with over 45 universities, e.g. Karlsruhe, Stuttgart and Strasbourg.

1.2. IRS

The *Institute for Reactor Safety* (IRS) is one of the three remaining institutes, which deal with nuclear engineering. It is divided into four departments with different fields of activity:

- Plant safety and system simulation
- Experiments and structure mechanics
- Fusion and radiation physics
- Neutron Physics and Reactor Dynamics

Over all, 70 employees work in the different departments.

The IRS contributes to the *European Nuclear Safety Research Program*. It concentrates on experiments and theories of severe accident consequences, the qualification of coupled codes for safety analysis of existing reactors, calculation of core-destroying processes, development of numerical models and experiments of bubble flows, and experiments to understand the process of steam explosions. Other activities are development and qualification of neutronic calculation methods and data libraries, development and qualification of coupled neutronic and thermo hydraulic codes, and design and safety studies of accelerator driven sub-critical reactors.

In addition, the IRS is involved in the *European Fusion Technology Program* with its objective to develop the fusion demonstration reactor ITER (International Thermonuclear Experimental Reactor) and an intense neutron source for fusion reactor material irradiation called IFMIF (International Fusion Materials Irradiation Facility). The IRS focuses on fusion neutronics, the neutron source IFMIF and the magnet safety.

The FZK and the IRS in cooperation with the CEA (Commissariat à l'Energie Atomique, France) hold a yearly summer school, the Frédéric Joliot/Otto Hahn (FJOH) Summer School on Nuclear Reactors, Physics, Fuels and Systems. The FJOH School alternates between Karlsruhe and Cadarache.

The IRS organizes a weekly seminar on reactor physics and related subjects. Scientists from the FZK and external institutes participate and present their work.

The internship was integrated in the department of *Neutron Physics and Reactor Dynamics* (NR) under the leadership of Dr. Cornelius Broeders. The NR department contributes at the nuclear safety program NUKLEAR and the fusion program FUSION. The department only focuses on numerical simulations. Therefore, the IRS has its own computer cluster to perform parallel computer jobs in order to reduce calculation time. In addition, it has access to PCU-time of the FZK Institute for Scientific Computing. The NR is a quite international department. Only a small part of the staff is German. Scientists from all over the world meet, e.g. Israel, Netherlands, Spain, Italy, and Romania. Therefore, the meeting language is consequently English. The NR and the IRS are trying to enhance the knowledge transfer to young scientists. Therefore, numerous interns, postgraduates and post-docs work in the institute.

Tutor of the work was Dr. Victor Hugo Sanchez Espinoza, who is a specialist for thermo hydraulic physics. The part of the work that deals with neutronic physics was done under guidance of Mr. Broeders, specialist for neutronic physics and the neutronic modular code system KAPROS. The IRS provided a Windows workstation for thermo hydraulic calculations and an access to the cluster for neutronic and coupled calculations.

Chapter 2

GENERAL DESCRIPTION OF THE SIMULATION OF GKN II

2.1. Description of the Reactor

In this project, the German pressurized-water reactor (PWR) in “Neckarwestheim” (GKN II) type KONVOI was studied. The Framatom Benchmark specifications were used, see [Ref.V]. GKN II with its 193 assemblies has a thermal power of 3850 MW and an electric power of 1350 MW. The fuel assembly consists of 300 fuel rods and 24 guide-tubes.

The GKN II reactor is a quite normal PWR. The cylindrical pressure vessel of the reactor can be divided into three parts. The coolant enters the vessel by the lower plenum. Then, it rises up to the active part, where it passes the rod assemblies and is heated up. The coolant leaves the vessel by the upper plenum.

Only the part of the core, which contains the active fuel rods, was simulated, even if COBRA-TF, as a strong tool, is able to simulate the upper and lower plenum of the reactor vessel. In axial direction the problem was divided into 10 levels with equal height ($\Delta h=0.39$ m). The point of origin of the axial coordinates was set at the bottom of the rods. The number of axial slices is a freely chosen variable. The more levels there are, the more the results will be exactly and the simulation time last. No flow blockages like grid spacers are simulated in the active part.

2.2. Core

To facilitate the problem and to reduce the computer costs only one eighth of the core was modeled, that is to say 31 assemblies (channels). For this, symmetries were used. **Figure 2-1** shows one eighth of a horizontal cut of the core. The diagonal and lower borders are symmetry lines. Afterwards the results can be used to characterize the whole core.

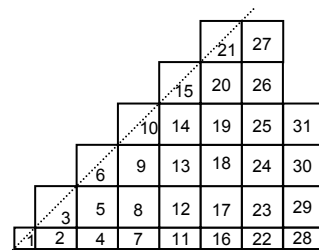


Figure 2-1: 1/8 of core

Bypass flow was neglected in these simulations. A possible bypass would be non-heated coolant, which passes between the assemblies or behind the reflectors, which are placed at the border of the core. The relative radial power distribution (**Figure 2-2**) was taken from a CASMO-data sheet (see **Appendix B**) [Ref.VI] calculated for this kind of reactor core.

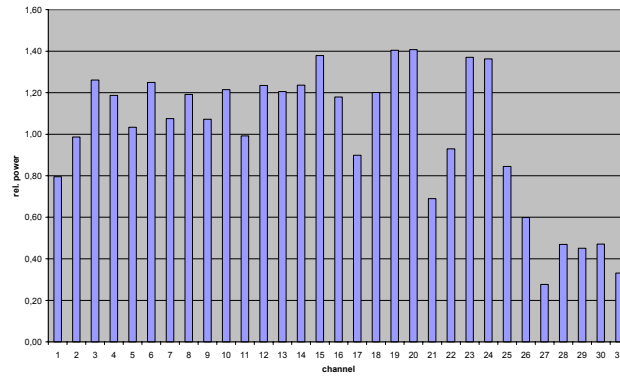


Figure 2-2: CASMO-data for radial power

There are three different types of channels: a complete channel (I), a half of a channel (II) and a quarter (III) with different characteristics. Each flow was calculated with the global flow through the reactor core.

Channel type	flow area [m ²]	wetted perimeter [m]	flow [kg/s]
I	2,993E-02	9,670	96,798
II	1,497E-02	4,835	48,399
III	3,742E-03	1,209	12,100

tab. 2-1- channel types for core simulation

2.3. Assembly

For the same reason as for the core simulation, only one eighth of the assembly was designed, i.e. 41 fuel rods and four guide-tubes. The rods were set up in a rectangular grid. This led to 90 subchannels. Each fuel rod is made up of a pellet of UO₂, a clad of Zircaloy 4 and a gap in between. The guide-tubes were represented by fuel rods with zero power, which is practically not true but facilitated the simulations.

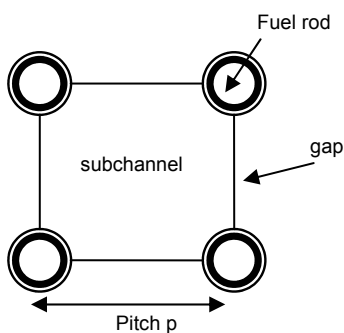


Figure 2-3: subchannel

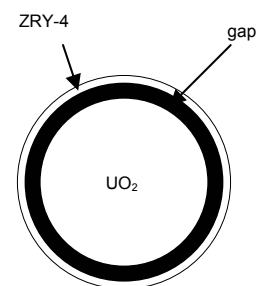


Figure 2-4: fuel rod

Figure 2-5 shows a horizontal cut of an assembly. The diagonal border is a symmetry line, just like the border on the right side. The border on the bottom is a real assembly border. The subchannels are classified in seven different types I-VII (see Figure 2-5) with different flow areas, flow quantities and wetted perimeters (see tab. 2-2). The flow quantities are calculated with the global flow through the reactor core.

Special attention should be paid at channel types V and II. They are located next to a real assembly border, so that their flow area is larger compared to types III and VII. The distance between two assemblies is larger than the pitch: $x=7.05E-3m$ and $p/2= 6.35E-3m$

Channel type	flow area [m ²]	wetted perimeter [m]	flow [kg/s]
I	9,041E-5	2,985E-2	2,924E-01
II	5,409E-5	1,492E-2	1,749E-01
III	4,520E-5	1,492E-2	1,462E-01
IV	4,520E-5	1,492E-2	1,462E-01
V	1,599E-5	0,373E-2	5,171E-02
VI	2,705E-5	0,746E-2	8,746E-02
VII	1,130E-5	0,373E-2	3,654E-02

tab. 2-2 – channel types for assembly simulation

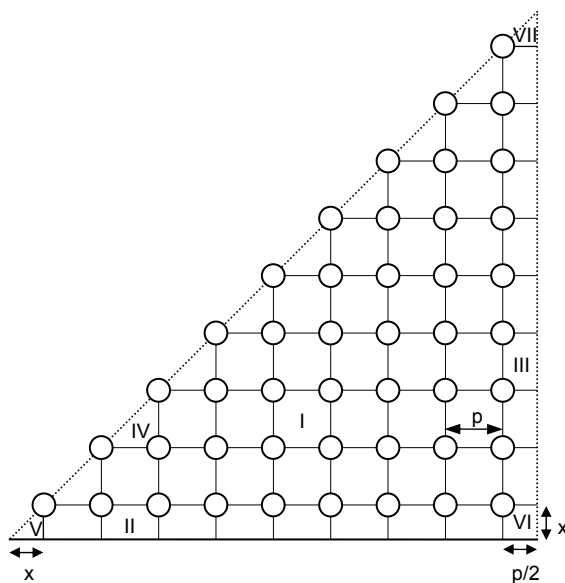


Figure 2-5: 1/8 of an assembly

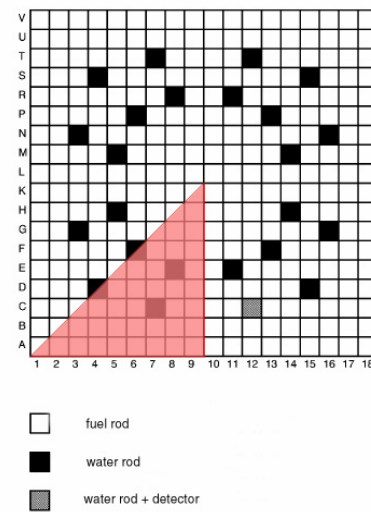


Figure 2-6: full assembly

The relative rod power was calculated with KARBUS for a first essay (see Figure 2-7). The rod numbering is taken from COBRA-EN and TF since it is the same. Later in Chapter 5 the relative rod power is one part of the coupling.

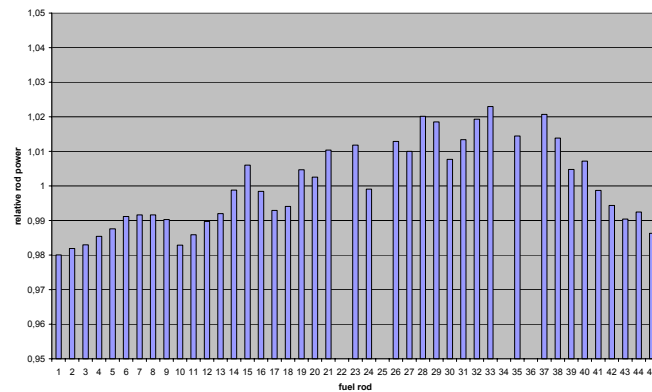


Figure 2-7: relative rod power

The following tables **Tab.2-3** and **Tab 2-4** specify the geometry data for GKN II reactor. **Tab 2-3** defines reference values for a normal, full power reactor situation. These values were used to calculate amongst others the boundary conditions (inlet flow, inlet coolant temperature etc.) and the average power of a fuel rod.

Tab. 2-3 Reactor data:

Reactor data		
Reactor thermal output	MW	3850
Electric power	MW	ca. 1350
Number of fuel assemblies in core		193
Power per dm ³ reactor core	kW/dm ³	ca. 95,3
Average fuel power per kg U ca (18x18-24)	kW/kg	. 37,4
Mass flow rate in core	kg/s	18682
Inlet temperature (full power)	°C	292
Outlet temperature (full power)	°C	325,5

Tab. 2-4 General Data for one rod assembly:

Fuel assembly data (cold geometry, 20 °C)		
assembly-identification		18x18-24 Uran
Assembly data		
Assembly edge length incl. water gap	cm	23.000
Pitch (fuel rod distance)	cm	1.270
Fuel rod data		
Pellet diameter	cm	0.805
Number of fuel rod in an assembly		300
Active rod length	cm	390.0
Cladding-tube inner diameter	cm	0.822
Cladding-tube outer diameter	cm	0.950
Cladding-tube material		ZRY-4
Guide-tube data		
Number of guide tubes per assembly		24
Guide-tube inner diameter	cm	1.110
Guide-tube outer diameter	cm	1.232
Guide-tube material		
Fuel assembly data (hot geometry, 310 °C)		
Active rod length	cm	391.56
Assembly edge length incl. water gap	cm	23.116
Pitch (fuel rod distance)	cm	1.272
Cladding-tube inner diameter	cm	0.822
Cladding-tube outer diameter	cm	0.950
Guide-tube inner diameter	cm	1.1127
Guide-tube outer diameter	cm	1.235

Tab. 2-5 Reference values for max. power reactor condition:

	Reference values
specific rod power: q' (W/cm)	170.5
Bore concentration in ppm $B_{nat} : C_B$ (ppm)	500
moderator temperature: T_m (°C)	310
clad-tube temperature: T_c (°C)	332.8
fuel temperature (average): T_f (°C)	500
pressure of cooling liquid: p (bar)	158

Chapter 3

THEORETICAL BASIS

Depending on the analyze scale a core or an assembly simulation is performed.

3.1. A thermo hydraulic subchannel analysis

The COBRA-TF [Ref.ix] and COBRA-EN [Ref.vii] codes are subchannel analysis tools. These tools are at the bottom of the simulation scale, i.e. they can be used to perform pin-by-pin thermo hydraulic calculations. The simulated volume is divided into several parallel channels. In each channel properties like temperature, density or pressure, only depend on the axial height. Cylindrical rods and gaps delimit these subchannels (see **Figure 2-3**). Gaps can be opened or closed: in a first case, interaction between the channels called cross flow is possible, in a second not. Open channels are often used for PWR, separate channels for Boiling Water Reactor (BWR).

3.2. A thermo hydraulic core analysis

With both codes, a simulation of the whole reactor core is possible. The assemblies are represented by an averaged channel containing the respective fluid, wetted and heated perimeter and pin power.

Pin by pin calculations can be interesting to locate hotspots in a fuel assembly, which represent a safety factor. The best case is a uniform temperature distribution. In the past, when an adequate computer power was not available, a simple core analysis was performed. Afterwards, for the assembly with the highest power a pin-by-pin calculation was made. In the future, a completely pin-by-pin analysis of the reactor core may be possible.

3.3. Theoretical background of COBRA-EN

The COBRA-EN code was developed as an upgrade of the COBRA-3C/MIT [Ref.vii] code in the 80's. It is used for Thermal-Hydraulic Analyses of Light Water Reactor Fuel Assemblies or Cores. Both, transient and steady state analyses are possible.

The underlying principles of this code are several theoretical models. A small part is presented here, the other part can be found in reference [Ref.vii]. In general, a thermo hydraulic code is based on a Flow Field Model, which describes the mass flux of liquid and vapor through the system and a Heat Transfer Model, treating the heat flux inside the fuel rod and the heat exchange with the coolant.

3.3.1. Flow Field Model

The COBRA-EN Flow Field Model is based on the conservation of mass, energy and momentum vector of a two-phase flow, i.e. a three-equation model. The differential conservation equations lead to a finite-difference equation system, which is solved. These balance equation are set up for the mixture mass and energy of the two-phase flowing coolant (two field flow: liquid and steam/void fraction). Momentum equations are divided into axial and lateral momentum. COBRA-EN has an option to calculate the void fraction directly from the vapor continuity equation, so to switch to a four-equation model. The Mass Balance, Energy Balance and Momentum Balance equations are given in **Appendix A**.

3.3.2. Heat Transfer Model

The Heat Transfer Model consists of a model for the heat conduction inside the rod and of a model for the heat exchange between rod and coolant.

3.3.2.1. Fuel Rod Heat Conduction

By using the fuel rod heat conduction model, the temperature distribution in the cylindrical fuel rod is calculated at each axial level. Axial heat conduction is negligible compared to the radial direction. The heat balance equation in radial direction is approximated with a first order finite-difference equation:

$$\left(\rho C_p V\right)_i \frac{\partial T_i}{\partial t} = Q_{i-1,i} + Q_{i+1,i} + Q_i''' V_i \quad (0.1)$$

ρ	fuel or clad density (kg/m ³)
C_p	fuel or clad specific heat (J/kg/K)
V	node volume
T	temperature (K) at the computational point
$Q_{i-1,i}$	$-k\partial T / \partial r _{r=r_{i-1}}$ = heat flow from node (i-1) to i (J/s)
$Q_{i+1,i}$	$+k\partial T / \partial r _{r=r_i}$ = heat flow from node (i+1) to i (J/s)
Q_i'''	volumetric heat generation rate (J/s/m ³) (fission power)

The fuel rod consists of the fuel pellet, the clad and a gap. Five nodes are reserved for the fuel pellet, two for the clad (Figure 3-1)

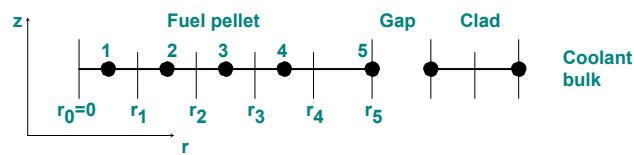


Figure 3-1: fuel rod mesh

3.3.2.2. Surface Heat Transfer

The Surface Heat Transfer model describes the exchange of heat between clad and coolant liquid. Depending on the temperature of rod and fluid, several relations are possible: single-phase forced convection, subcooled nucleate boiling, saturated nucleate boiling, transition and film boiling (post CHF boiling).

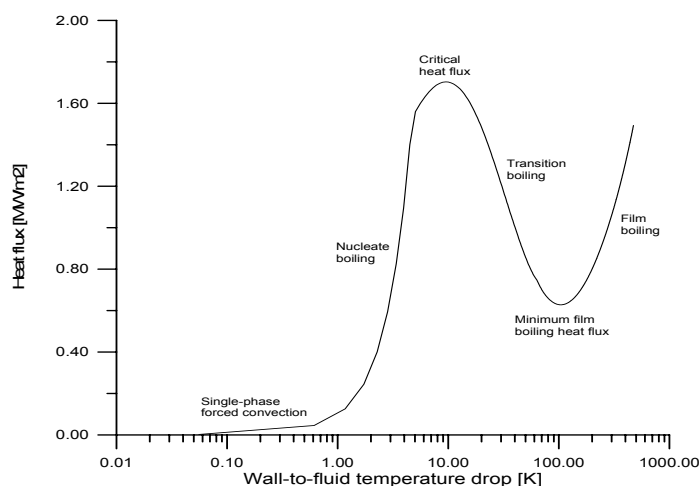


Figure 3-2: heat flux as function of superheat

The general relation for the heat transfer is:

$$q'' = H(T_w - T_b) \quad (0.2)$$

Where q'' is the heat flux, H the rod-to-coolant heat transfer coefficient, T_w the surface temperature and T_b the fluid temperature. The heat transfer model determines the flux or the coefficient H .

In a PWR only single-phase forced convection and nucleate boiling (Thom correlation) appear, except in case of an accident like LOCA (lost of coolant accident). The heat transfer coefficients of the liquid phase forced convection and nucleate boiling are given in **Appendix A**.

3.4. Theoretical background of COBRA-TF

The COBRA-TF (**Coolant Boiling in Rod Arrays – Two Fluid**) code was developed at the Pacific Northwest Laboratory under sponsorship of the United States Nuclear Regulatory Commission to provide best-estimate thermal-hydraulic analyses of a light water reactor [Ref.viii]. It was designed to treat particularly lost-of-coolant-accidents (LOCA) of PWR and rod bundle accidents of LWR.

COBRA-TF provides a three-field description of a two-phase flow. For each field, i.e. vapor, continuous liquid, and entrained liquid drops, a set of conservation equations is solved. Just as defined in section 3.3, these equations are mass, energy and momentum conservation. The use of an extra field is exceptional for this kind of codes. As entrained droplets have a quite different behavior than continuous liquid or vapor, this extra field is necessary. The interaction of liquid and vapor cannot be adequately described with a set of average liquid-phase equations. This extra field favors the use of COBRA-TF for BWR or accidents causing boiling in the reactor core.

3.4.1. Conservation equations

The Conservation equations consist of 9 equations. Four Mass Conservation Equations for vapor, continuous liquid, entrained liquid and noncondensable gas mixture are solved. The Energy Equations consist of one equation combining the liquid fields and one equation for a vapor-gas mixture. Finally, one Momentum Equation for each of the three fields is solved. The detailed explanation of these equations may be found in Thurgood, section 2 [Ref.ix]. These conservation equations are solved with the finite-difference method.

3.4.2. Heat Transfer Model

The Heat Transfer Model consists of multiple parts: Heat Conduction for the fuel rod, Surface Heat transfer, the gap conductance model and the quench front model. The first three models are annotated in the following. The quench front model is, because of its complexity, not mentioned. In addition, it is quite irrelevant for the analyzed problem since it deals with heat transfer below the critical heat flux. More information may be found in Thurgood, section 1 [Ref.ix]

3.4.2.1. Fuel Rod Heat Conduction

The conduction model for the fuel rod is similar to the model used in COBRA-EN (section 3.3.2.1) with the same nodding. The centerline temperature is obtained by Hermite interpolation.

3.4.2.2. Surface Heat Transfer

The Surface Heat Transfer model is analogous to the model used in COBRA-EN. At low surface temperatures single phase forced convection and nucleate boiling appears. The forced convection part is calculated for steam with the *Dittus-Boelter* correlation, the liquid with either the *Dittus-Boelter* correlation for turbulent flow or with a laminar flow correlation (see **Appendix A**).

The nucleate boiling part is determined by the *Chen* correlation. For this case, the rod temperature has to be greater than saturation but less than the critical heat flux. Liquid has to be present. This relation concerns to the saturated nucleate boiling region and the two-phase forced convection region. The *Chen* correlation uses a superposition of a forced convection, described by *Dittus-Boelter*, and a pool boiling relation. The pool boiling part is determined by the *Foster-Zuber* equation. For detailed information see reference [Ref. ix], volume 1.

3.4.2.3. Gap Conductance

The heat transfer in the gap between fuel pellet and clad consist of three terms. It is caused by radiant heat transfer, described by the *Stefan Boltzmann* equation, convection with filled-in gas or physical contact of pellet and clad.

Chapter 4

SIMULATIONS

Both codes, COBRA-EN and COBRA-TF, dispose of a textual input. That means that the user, who wants to perform a simulation has to create a text file with a precise defined order and form. Special attention has to be paid at the length of values (e.g. 8 byte) and the line length. The text file must contain all of the important data. The codes scan the input file for characteristic signs, which identify the following data. If the data has not the expected form, the code announces an input error. Both codes give an input feedback, which is very useful to detect input errors.

4.1. Simulations with COBRA-EN

Two different kinds of simulations were performed: an assembly and a core analysis. The Compaq Visual Fortran Developer Studio was used to compile and run the COBRA-EN code. Input and output data can be given in SI or British/American Units.

4.1.1. Assembly analysis

The 55 subchannels and 45 fuel rods were shaped with a special numbering (Figure 4-1). This numbering is quite important because it differs from the numbering of COBRA-TF. COBRA-EN allows declaring the right side and diagonal border as symmetry axes. Flow area, wetted (heated) perimeter and neighbor channels were defined for each channel with indication of gap width and distance of the channel centers. Rod specifications like the geometry, material properties of the clad and of the UO₂ and rod-to-channel-connections data were fixed. The Automatic Generation of Connection Data of COBRA-EN was not used since it handles rectangular assemblies as a whole and so does not use symmetries.

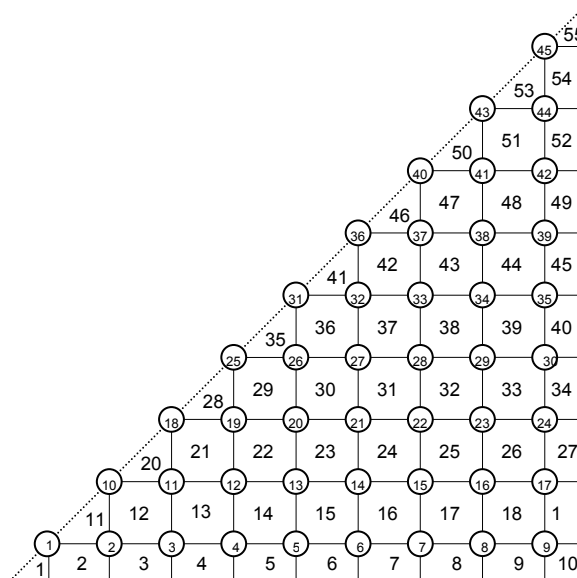


Figure 4-1: CobraEN numbering

For the assembly analysis, a subchannel analysis with the COBRA three-equation model (mixture mass, energy and momentum) was chosen. Since no strong boiling was expected, the COBRA four-equation model, which takes the vapor mass into account, was not necessary. The chosen heat

transfer model considers only single phase convection (*Dittus-Boelter* correlation) and nucleate boiling (*Thom* correlation), i.e. a boiling curve up to the critical heat flux (CHF) point (see **Figure 3-2**). For the turbulent mixing model, the following relation was chosen:

$$w'_k = a s_k G_k$$

w'_k =	turbulent cross flow (kg/m/s) through gap k
s_k =	gap width (m)
G_k =	axial mass flux around gap k (kg/m ² /s), computed as the average value in channels I and I', i.e., ($m_I+m_{I'}$)/($A_I+A_{I'}$),

The coefficient **a** had to be changed in the source code from 0.02 to 0.01 for a comparison with the results of COBRA-TF (see section 4.2.1.3). Boundary conditions were set at the bottom of the simulation area, viz inlet temperature and mass flux per area. The power distribution of the fuel rod has a sinusoidal shape in axial direction and is radial depended. The radial distribution is calculated preliminary by a neutronic code (see **Figure 2-7**).

In a first run, closed channels are favored, in a second run, opened channels.

4.1.1.1. Results for closed channel analysis

The closed channels inhibit cross flow, so that there is no heat exchange between different channels and significant temperature gradients are achievable. The graph (**Figure 4-2**) shows the fluid exit temperature for every channel. Obviously, the temperatures differ depending on the channel. This effect is due to the radial power distribution, to different flow areas, and to the presence of water rods. Channels 1-10 are placed at the outer border of an assembly. Therefore, their flow area is larger comparative to an inner channel: +41% for channel 1 and +20% for channels 2-10. This means that a bigger amount of fluid is heated with the same heat flux. As a result, lower temperatures are reached at the outlet. If a channel is neighbored to a water rod, the respective heat flux and the exit temperature are smaller (channels 24, 25, 28, 29, 31, 32, 35, 38, 39, 41, 42, 43, 44, 46). The radial dependence of the power distribution has a smaller impact on the temperature. It can be observed for example for higher channel numbers; the outlet temperature decreases slightly.

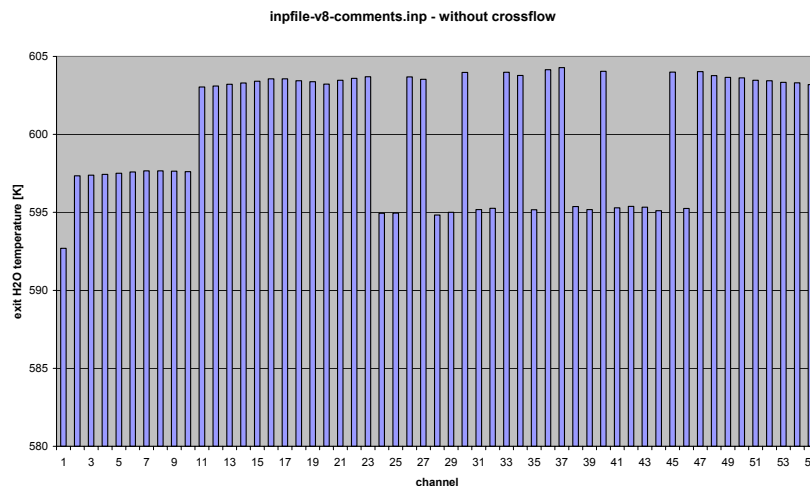


Figure 4-2: COBRA-EN assembly simulation without crossflow - coolant outlet temperature

The results were post processed after the calculation in order to obtain **average values for each rod**. **Figure 4-3 - Figure 4-7** have plausible characteristics for the selected representative rods in axial dependence. The liquid temperature increases from its inlet value of 565K to a maximum value of about 563K to 604K. Due to the heating up of the fluid, its density declines from 7.45g/cm³ to 6.5-6.6g/cm³. This means, density declines more than 10 percent.

The clad temperature shows a displacement of the maximum in upper direction while the pellet temperature is nearly symmetrical to the middle of the fuel rod. This effect is explicable by the fact that the coolant flows in upper direction and is heated up meanwhile. The fluid is less refrigerant in the upper part.

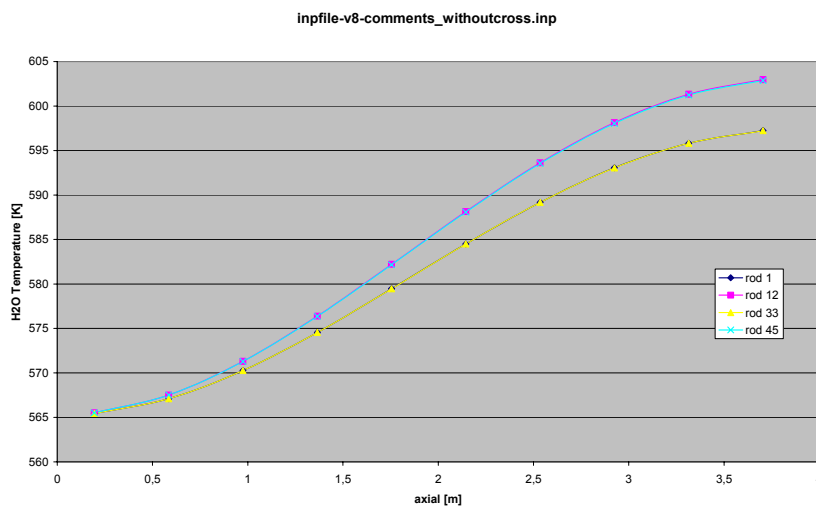


Figure 4-3: COBRA-EN assembly simulation without crossflow - coolant outlet temperature

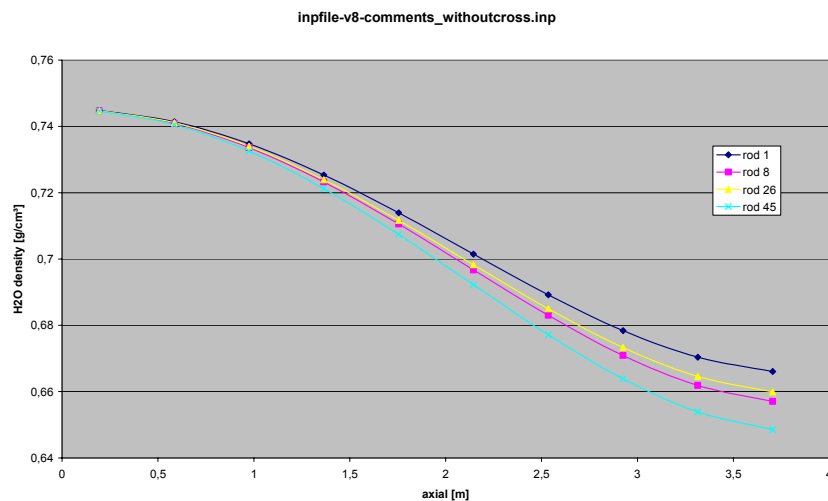


Figure 4-4: COBRA-EN assembly simulation without crossflow - coolant density

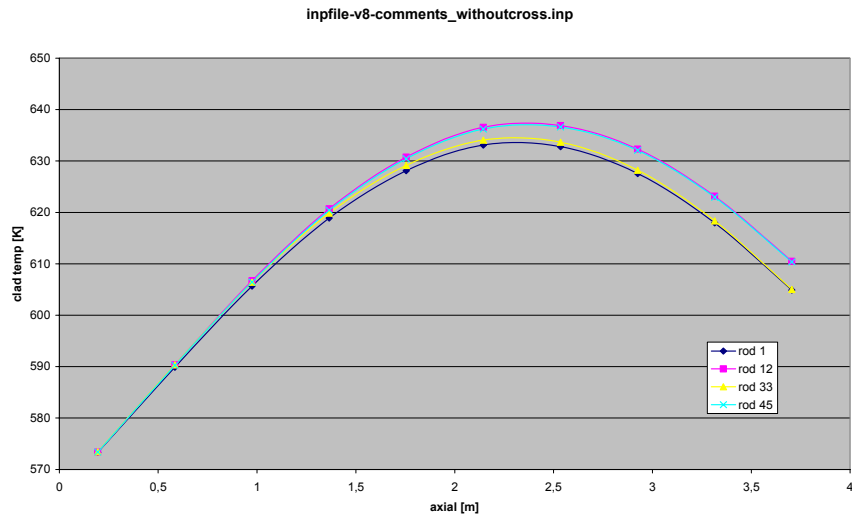


Figure 4-5: COBRA-EN assembly simulation without crossflow - clad temperature

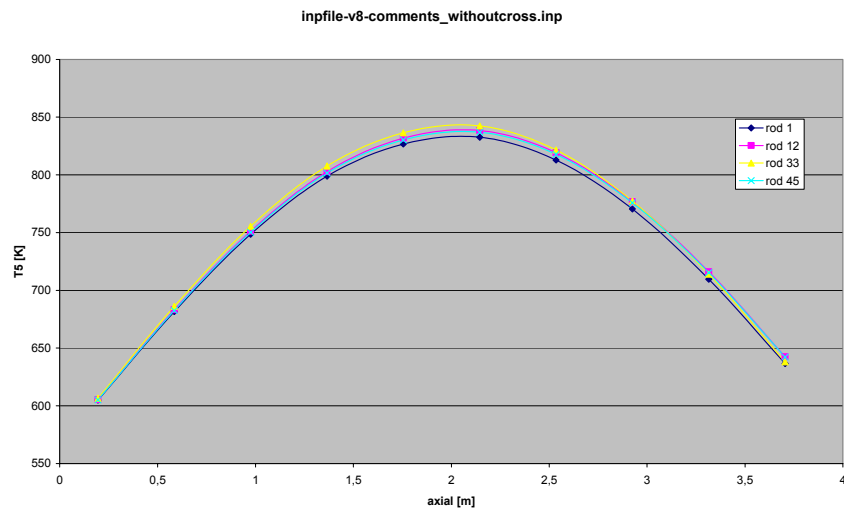


Figure 4-6: COBRA-EN assembly simulation without crossflow - outer pellet temperature

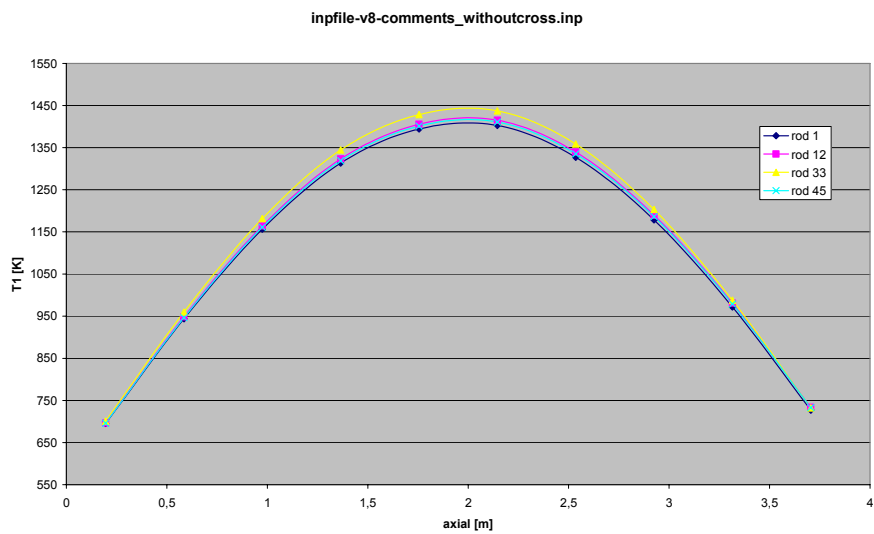


Figure 4-7: COBRA-EN assembly simulation without crossflow - inner pellet temperature

4.1.1.2. Results for open channel analysis

This time, an open channel analysis was performed. The mayor difference to the first simulation is that strong temperature gradients between neighboring channels are not possible. Appearing cross flow between these channels harmonizes in a certain manner the temperatures.

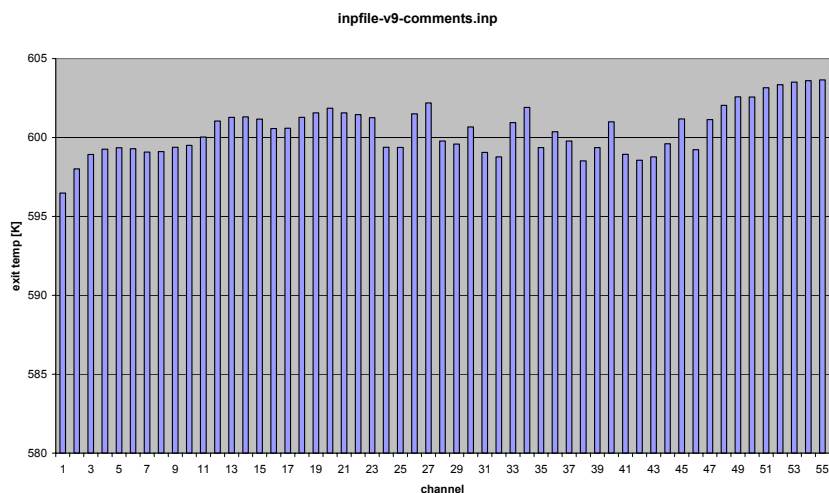


Figure 4-8: COBRA-EN assembly simulation with crossflow - outlet coolant temperature

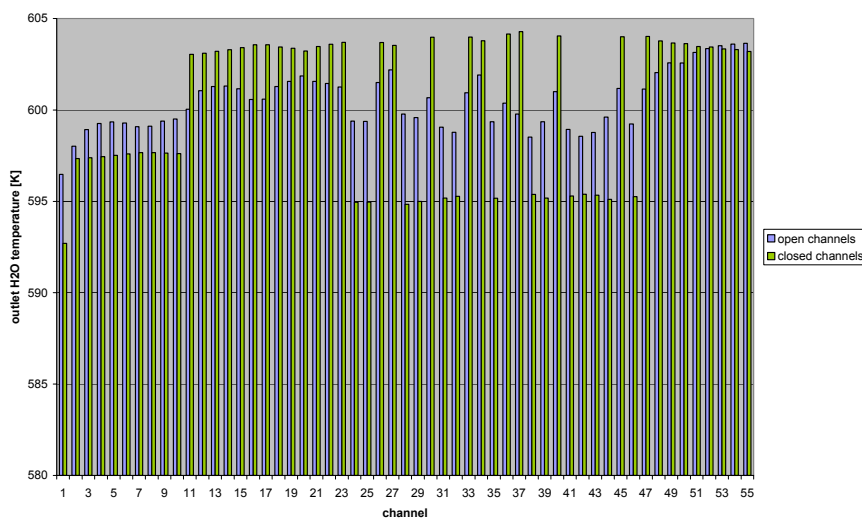


Figure 4-9: COBRA-EN assembly simulation - comparison open/closed channels

The Figure 4-9 shows how the outlet temperatures change. There is a strong impact on border-channels and those, which are neighbored to a water rod. Their temperature increased significantly, e.g. for channel 29 from 595K to ~598K. Due to this harmonization of the coolant temperature, the other characteristics like density and fuel temperature change too, but less obviously. The impact on the inner fuel temperature is very weak. The cross flow between the channels helps to obtain a constant temperature profile at the outlet of the core vessel, to reduce temperature peaks.

Coolant temperature and density, clad temperature, and outer and inner pellet temperature are attached in Appendix C.

4.1.2. Core analysis

COBRA-EN is able to simulate a whole core as mentioned before. The input data for a core and an assembly simulation are quite similar. For the core simulation, 31 channels were shaped (see **Figure 2-1**). The power was defined directly for each assembly, i.e. for each channel, and not for the fuel rods. Two simulations were done, the first with a homogenous, the second with an inhomogeneous radial power distribution.

4.1.2.1. Results for homogenous radial power distribution

The outlet coolant temperature is constant at ~ 600.5 K for all fuel assemblies (see **Figure 4-10**). That all the assemblies have the same temperature profile is plausible as they have all the same flow-area to rod-power relation, unlike the assembly simulation (see section 4.1.1).

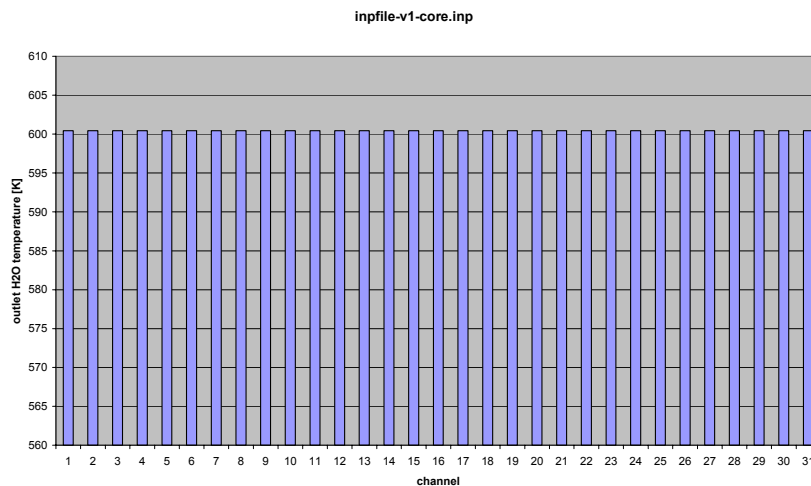


Figure 4-10: COBRA-EN core simulation (no radial dependency) - outlet coolant temperature

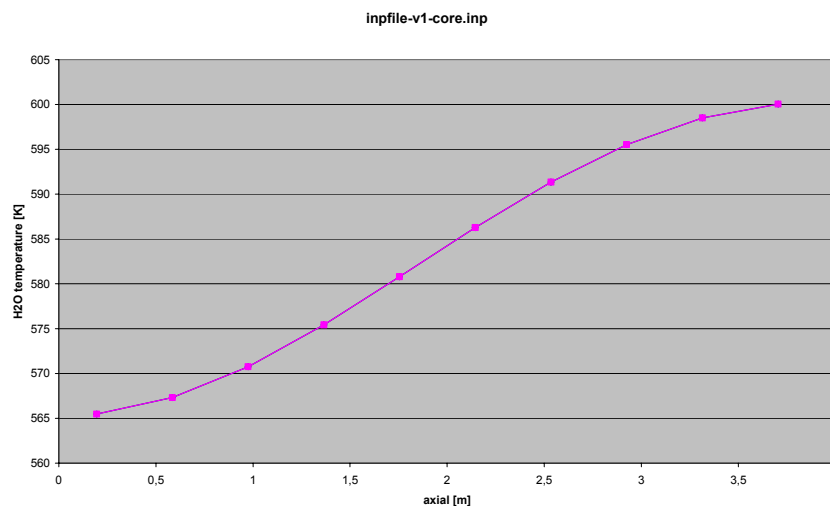


Figure 4-11: COBRA-EN core simulation (no radial dependency) - coolant temperature

4.1.2.2. Results for non-homogenous radial power distribution

The second core simulation was adapted to the CASMO-Data (see **Appendix B**) for this kind of reactor core. The outlet coolant temperature **Figure 4-12** reflects in a good way the radial power distribution (see

Figure 2-2). Some deviations might be noticed for channel 19 and 20 for example. This may be due to cross flow.

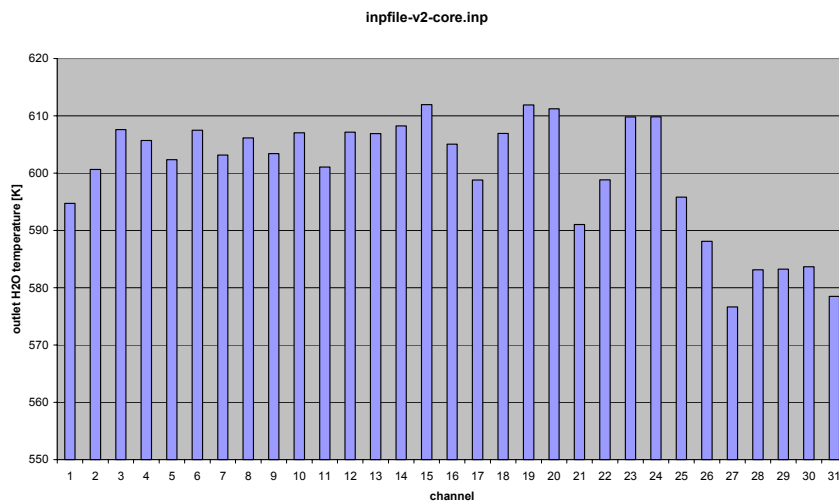


Figure 4-12: COBRA-EN core simulation (radial dependency) - outlet coolant temperature

4.1.3. Review on COBRA-EN

COBRA-EN has a relatively simple input data sheet. An assembly simulation consists of about 10 pages source code. It took about 1 week to implement the input data incl. debugging.

Due to the steady state option, the calculation time for this particular problem is very shortly (~5 sec).

4.2. Simulation with COBRA-TF

Just like for the COBRA-EN two kinds of simulations were performed, a core and an assembly analysis. The Compaq Visual Fortran Developer Studio was used again. Input for this code can be performed in either SI or British units. Output is compulsory in British units.

COBRA-TF does not directly supply a steady state calculation. Therefore transient simulations with a simulation time of 5 seconds were performed. After this time, a steady state situation was assumed, which seems to be justified through graphs **Figure 4-13** and **Figure 4-14**.

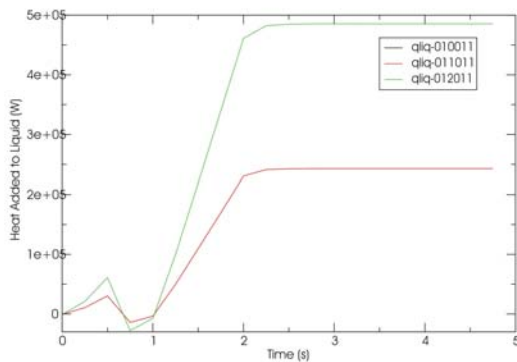


Figure 4-13: Heat added to Liquid for steady state verification

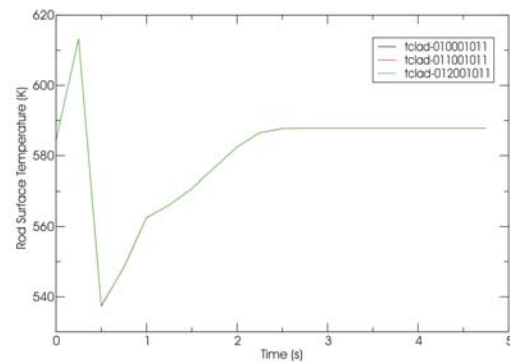


Figure 4-14: Rod surface temperature for steady state verification

4.2.1. Assembly analysis

The COBRA-TF input sheet consists of multiple information cards. In this section, some of these cards are described more precisely because they affect the coupling in **Chapter 5**. In general, the problem was shaped similarly to the COBRA-EN one. This means that it consists of 45 rods, 55 channels and uses right side and diagonal symmetry. However, in detail there are some differences. The geometry input is much more complex. Among other things, this may be, caused by the fact that COBRA-TF is able to simulate the upper and lower plenum of the vessel too. Several vertical sections can be specified in the channel description, even if in this simulation only one section was used (Group 4 in **Appendix E**). The numbering for the channels differs from COBRA-EN (**Figure 4-15**). Each gap between the channels was defined (**Figure 4-16**). To obtain a three-dimensional form of the transverse momentum equation, the straight-lined and the orthogonal connections were specified. (Group 3)

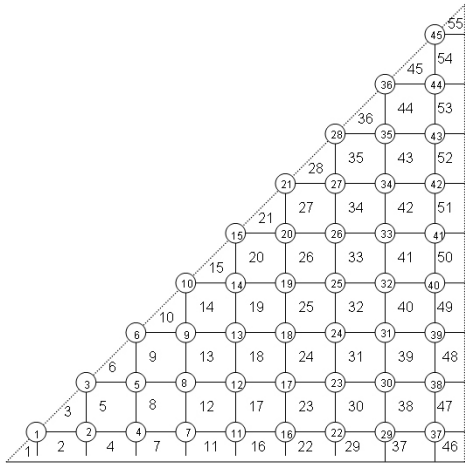


Figure 4-15: COBRA-TF channel numbering

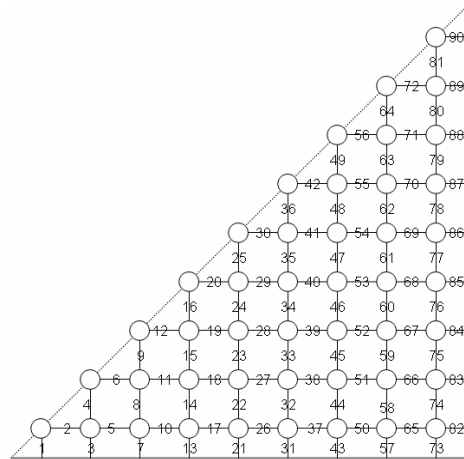


Figure 4-16: COBRA-TF gap numbering

In the fuel rod data part of the input file (Group 8), thermal rod-to-channel connection, gap conductance and a reference to an axial power profile were described. The axial profile consists of a certain number of axial points and relative power respectively. This profile is important for the coupling.

For every channel, upper and lower boundary conditions data were set (Group 10). At the bottom, pressure, enthalpy and inlet flow and on the top, pressure and enthalpy were defined.

A value of $a=0.01$ was chosen for the turbulence mixing coefficient. COBRA-TF uses the same turbulence mixing model as the one chosen for COBRA-EN.

Material properties for Uranium oxide (UO_2) and Zirconium (Zr) were set. The code proposes build-in properties, but to ensure that both codes use the same values the properties were redefined (data taken from COBRA-EN):

	density [kg/m^3]	specific heat [$J/kg/K$]	thermal conductivity [$W/m/K$]
UO_2	10970	242.672	3.46
Zr	6558	242.67	15.22

tab. 4-1 properties of UO_2 and Zr

The defined values are assumed constant while temperature changes, which is not a safe assumption.

The header file "respar.h", which contains the maximum values for the numeric array declaration, had to be modified because of the size of the problem, e.g. 45 instead of planned 30 fuel rods (see Appendix D).

An input data sheet is attached in Appendix E.

4.2.1.1. Results for closed channels

The first simulation had no cross flow, which means that large temperature differences between two channels are possible. Figure 4-17 shows the water outlet temperature. To facilitate the comparison to the COBRA-EN simulation later, a numbering similar to COBRA-EN was chosen for the presented figures. The position of the water rods are clearly visible (connection to channels 24, 25, 28, 29, 31, 32, 35, 38, 39, 41-44, 46). An effect due to comparatively larger flow areas can be observed for lower channel numbers; the temperatures are minor than in higher channels.

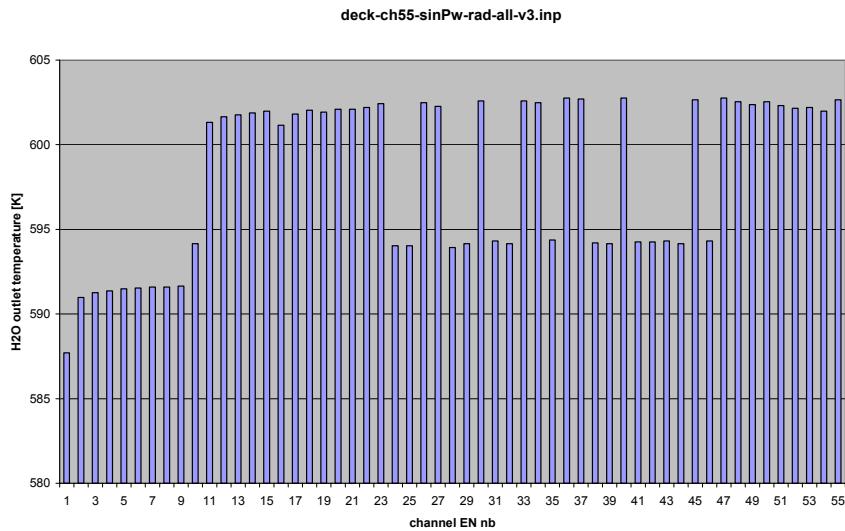


Figure 4-17: COBRA-TF assembly simulation without crossflow - coolant outlet temperature

Figure 4-18 and Figure 4-19 show water temperatures and densities. The temperature increases from 565K to ~594-603K. The density declines from 0.745 to 0.65-0.675 g/cm³. However, in the upper part of the vessel the temperature and density is quite noticeable. From a height of over ~3.4m on constant values are reached. Even if the heating power of the fuel rods at the upper end is minor, this should normally not appear. This effect is due to a global pressure loss at the top of the plenum, which may be caused by inappropriate boundary conditions. The velocity of the fluid is too high at the end of the channels. Expected was a linear pressure decrease, but Figure 4-20 clearly shows a different behavior. This is a real value-changing failure of this simulation because otherwise higher outlet temperatures and lower densities would be reached. To oppose, the upper plenum could be shaped. This would probably cause a linear pressure behavior in the vessel.

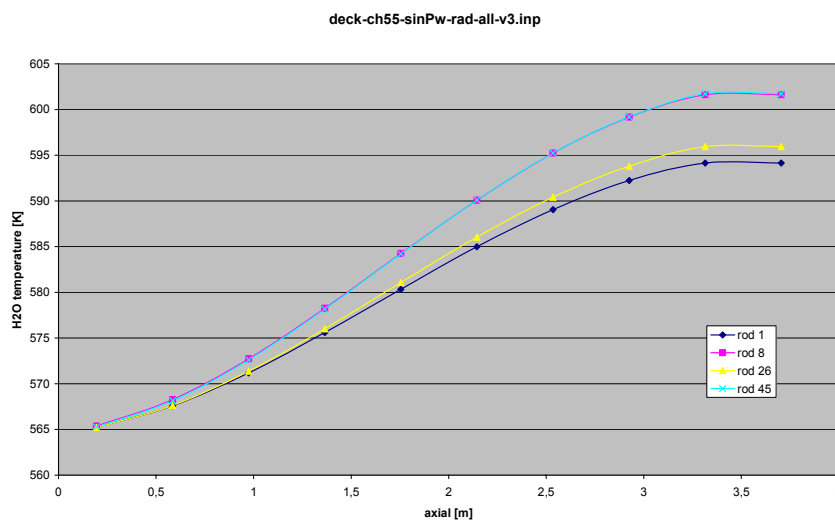


Figure 4-18: COBRA-TF assembly simulation without crossflow - coolant temperature

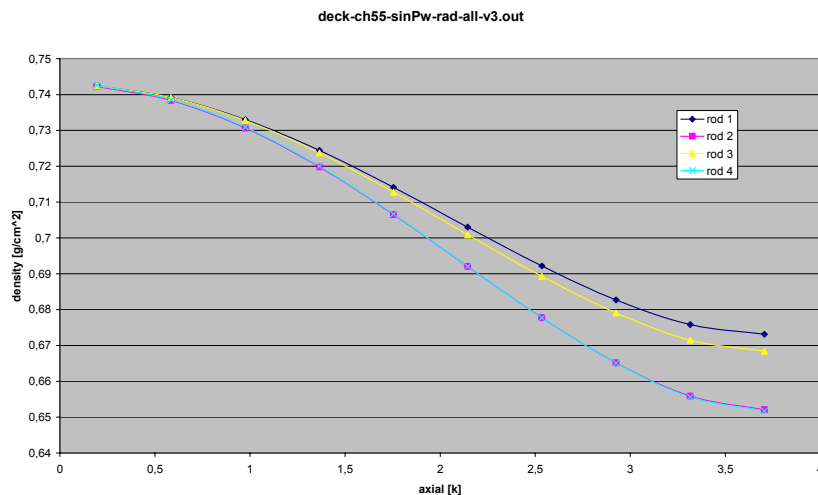


Figure 4-19: COBRA-TF assembly simulation without crossflow - coolant density

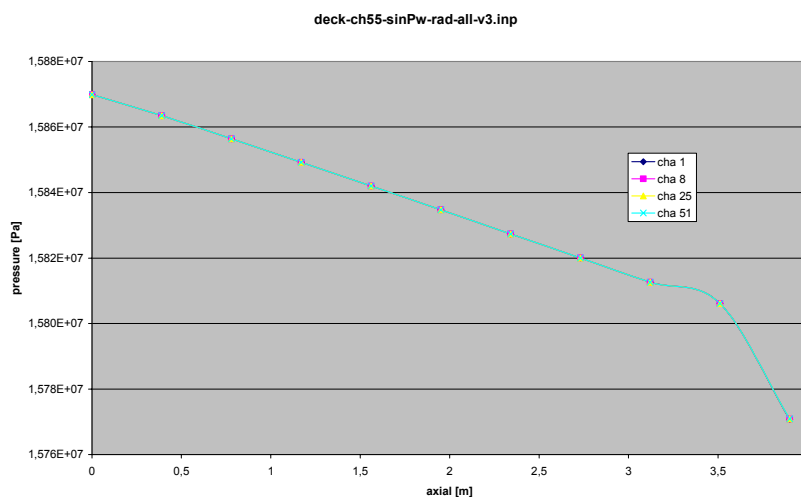


Figure 4-20: COBRA-TF assembly simulation without crossflow - pressure

4.2.1.2. Results for open channels

The second simulation with COBRA-TF included cross flow between two channels, i.e. turbulence mixing was enabled. The outlet water temperature is presented by Figure 4-21 while Figure 4-22 shows the differences to the closed channels simulation (section 4.2.1.1). The most important changes can be observed for lower channel numbers. Temperatures for channel 2-9 for example are lifted about 4 K. However, temperatures for the channels neighbored to a water rod did not change radically. It seems to be doubtful that temperatures for “lower” channels change quite significantly, but for other channels (with important temperature differences) the impact of cross flow is small.

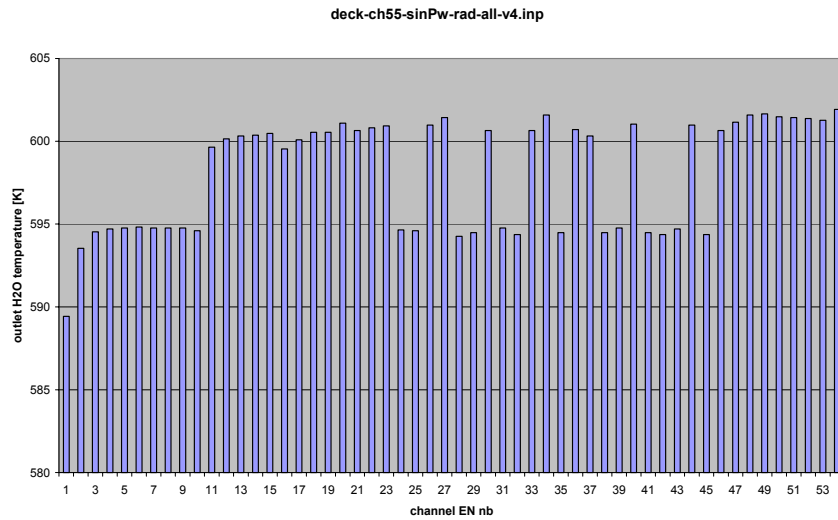


Figure 4-21: COBRA-TF assembly simulation with crossflow - outlet coolant temperature

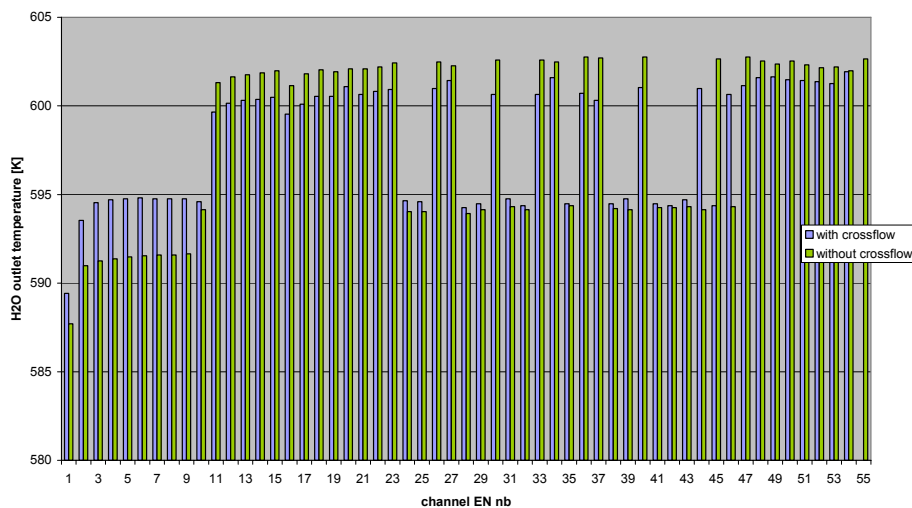


Figure 4-22: COBRA-TF assembly simulation - differences of outlet coolant temperature open/closed channels

4.2.1.3. Comparison to COBRA-EN

The differences between COBRA-EN and COBRA-TF for open channels are large (see Figure 4-8 and Figure 4-21). The outlet temperatures of COBRA-EN are much more harmonized than the ones of COBRA-TF. Probably this is due to COBRA-TF mixing model. Because of lack of experimental data, this cannot be verified. The focus will be on the comparison of closed channel systems.

Comparing COBRA-EN and COBRA-TF is not only interesting for code validation, but also to find possible modeling errors. Therefore Figure 4-23 points out the differences between the outlet temperatures.

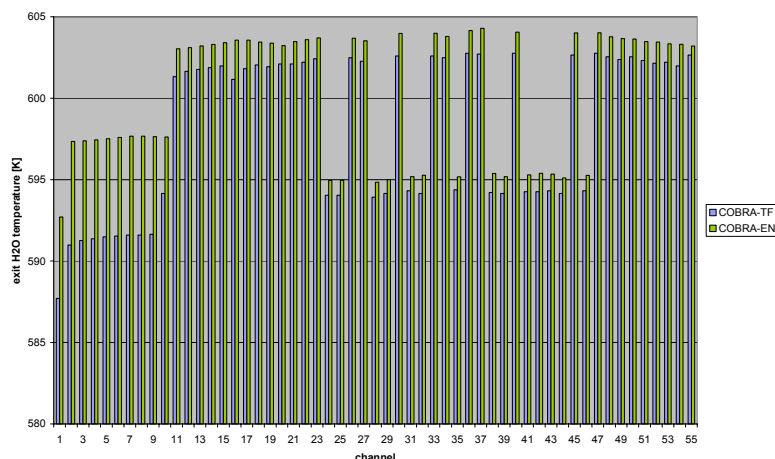


Figure 4-23: Comparison of outlet coolant temperatures from COBRA-EN and COBRA-TF

Two points can be stated. First, there is a continuous temperature difference for higher channels (11-55), but with the same profile. An explanation for the temperature discrepancy is given in section 4.2.1.1. Channel 16 seems to break ranks. This may be an indication for a mistake in the input sheet in COBRA-TF. Second, the differences for the “lower” channels (1-10) are relatively strong. Without any experimental data it is quite difficult to decide which simulation is wrong. Nevertheless, COBRA-TF has a sort of step for channel 10, which seems to be improperly because this channel has the same power-flowarea-relation as channel 9.

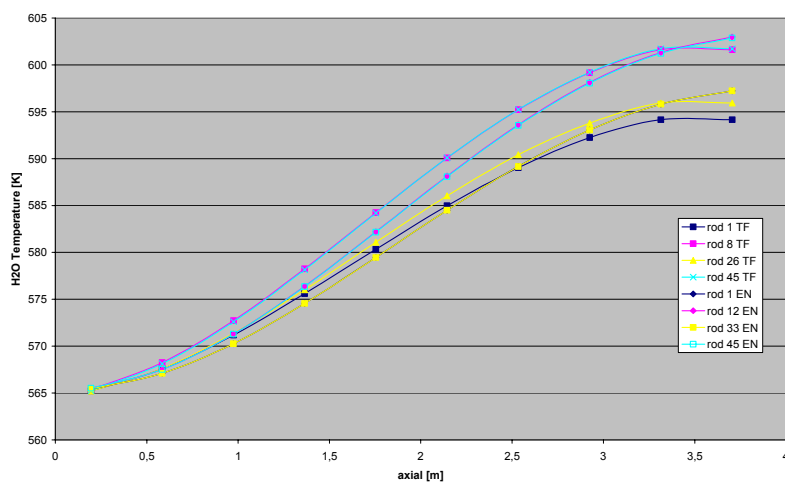


Figure 4-24: Comparison coolant temperatures from COBRA-EN and COBRA-TF

4.2.2. Core analysis

COBRA-TF has an option to represent multiple rods by one representative rod. This function was used for a core analysis where each channel includes one of these rods. The other input, e.g. gap or channel declaration was done in the same way, just like for an assembly analysis. The numbering is declared in section 2.2.

Just as for the EN-Simulation, two different simulations were performed, the first one without radial dependence of rod power, the second with.

4.2.2.1. Results for homogenous radial power distribution

A homogenous result for the outlet temperature at 589 K was obtained. The constant values can be explained (see above) with the constant rod power-flow area relation for all channels.

The plateau in coolant temperature chart (Figure 4-25) at the upper end of the vessel can be observed similar to the assembly simulation. This causes the difference in the outlet temperatures between COBRA-TF and COBRA-EN.

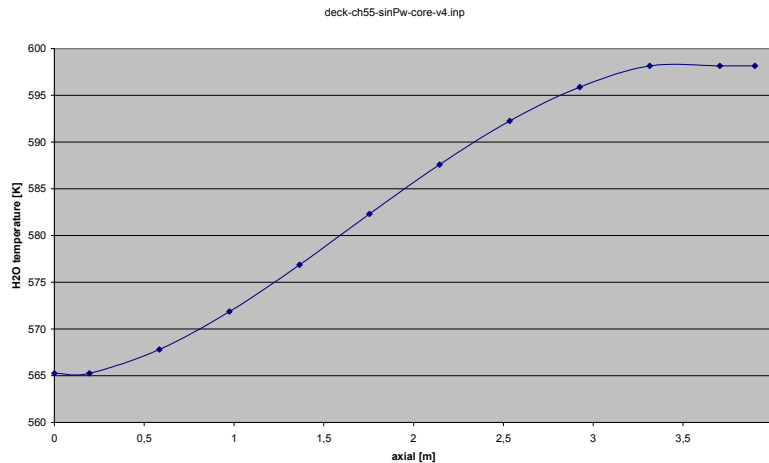


Figure 4-25: COBRA-TF core simulation (no radial dependency) – coolant temperature

4.2.2.2. Results for non-homogenous radial power distribution

A core simulation with the CASMO data (Appendix B) was performed. The profile of the outlet water temperature reflects this relative radial power distribution (Figure 2-2).

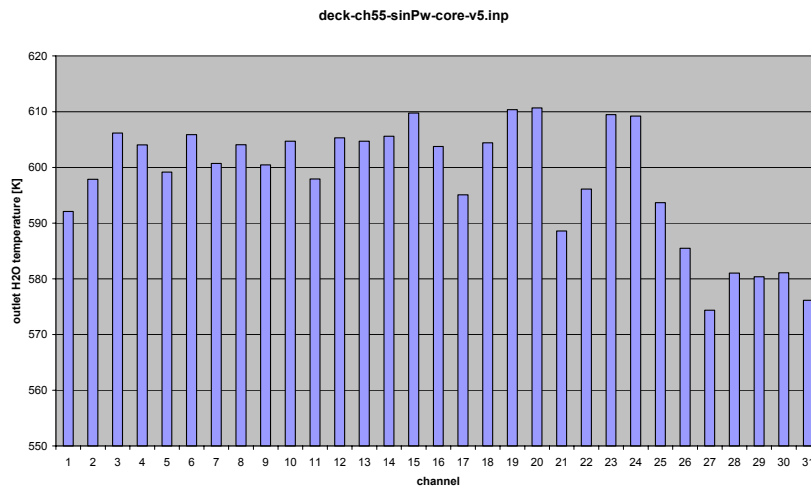


Figure 4-26: COBRA-TF core simulation (radial dependency) – outlet coolant temperature

4.2.2.3. Comparison to COBRA-EN

The Figure 4-27 shows in a good way the difference due to the plateau mentioned before. The COBRA-EN results are about 3 K higher than COBRA-TF otherwise the two results are very comparable.

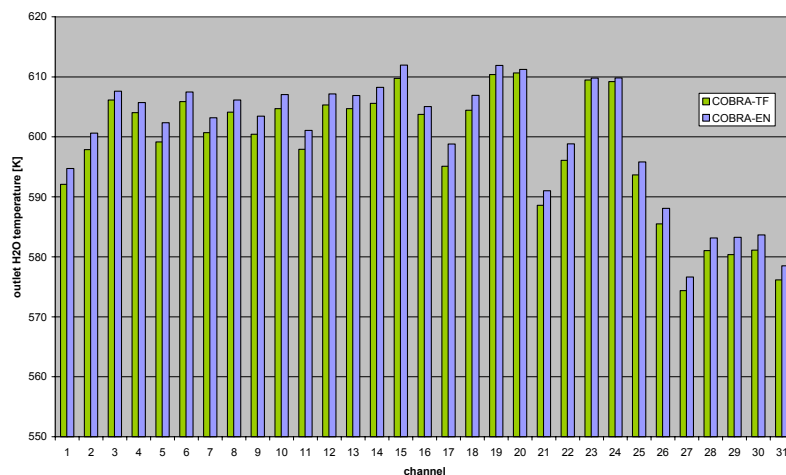


Figure 4-27: comparison of COBRA-EN/TF core simulation (radial dependency) – outlet coolant temperature

4.2.3. Review on COBRA-TF

COBRA-TF seems to be a very strong simulation tool. In comparison to COBRA-EN important improvements like the entrainment drops model were made. Nevertheless, there some comments need to be mentioned.

The COBRA-TF data input is much more complicate than the one for the EN-version. The different number of input pages can illustrate this: COBRA-EN ~10 pages, COBRA-TF ~42 pages. It took about 3 weeks to implement a working input file for COBRA-TF.

Some difficulties appeared while trying to fill the reactor vessel with water for the beginning of the simulation. In a first case, a void fraction of 0.001 and a fraction for liquid of 0.999 were tried, but this caused an error message. In the following, the simulation began with 100% steam and successive the vessel was filled with water in the simulation. This led to a very long simulation time. Finally, the void fractions were chosen as 1.0 and 0.999, which had the desired result that the vessel was filled from the beginning on with water.

To reduce input complexity, the upper plenum could be shaped. Every subchannel would end in this plenum and a single boundary condition could be declared. Unfortunately, only six channels can lead in the same upper channel. This means, for 55 channels 3 upper levels would be necessary.

A bug was found in the source code for the conversion from SI units to British units is performed (see Appendix F). In general, the output in British units demands an extra effort for the post-processing.

Due to the fact that COBRA-TF does not perform a steady-state simulation directly, calculation time is quite long; about 100 min on an IRS cluster PC.

A different turbulence mixing coefficient than $a=0.01$ has been tried, but COBRA-TF did not convert. Therefore, the coefficient in the COBRA-EN source code had to be modified.

Chapter 5

COUPLING OF COBRA-TF AND KARBUS

5.1. Introduction

Neutron and thermo hydraulic physics do influence each other in this kind of problem. Therefore, a coupling between a neutronic and a thermo hydraulic code seems to be reasonable. As seen before, the thermo hydraulic codes are able to calculate fuel temperature, clad temperature, water temperature and density for the 10 axial levels. These values are important for the neutronic calculation of the rod power. Clad, fuel and water temperature influence the neutron absorption via the Doppler Effect. The water density is important for the thermalization of neutrons. The more the water is dense, the more impacts will appear between hydrogen atoms and neutrons. There is a stronger thermalization and thus rod power is higher. In general, the rod power will not be sinus shaped. The neutronic code returns the calculated rod power to the thermo hydraulic code.

An exchange of axial and radial dependent data between the neutronic and thermo hydraulic code has to be realized. After a few iterations, a steady state solution is expected.

Coupled Neutronic codes with subchannel thermo hydraulic codes already exist. An example is NORMA-FP, which consists of QUARK (three-dimensional dynamics code), NORMA [Ref.iv] (three-dimensional burnup code) and COBRA-EN.

As mentioned before, the neutron physics simulation tools are divided into probabilistic and deterministic codes.

A probabilistic code simulates the journey of neutrons. That means, from their creation through fission, their scattering until their death through absorption or escape. At each event, i.e. collision with a coolant atom, the consequences are determined through the cross sections and a probabilistic factor. Millions of neutron trips are simulated and a neutron distribution is obtained. The user has to decide in advance, which properties he wants to obtain, as no post processing of the results is possible.

A deterministic code solves the neutron transport equation. Therefore, several assumptions have to be taken, like subdivision of the neutron energy scale into different groups with averaged cross sections. A neutron distribution is obtained from which several properties can be derived. The deterministic code is very fast for variation calculations.

In this case, the deterministic neutron physics code for burn-up studies KARBUS was used. KARBUS is a part of the modular code system KAPROS [Ref.X] which was developed in the FZK in the late sixties. KAPROS contains modules for all the important calculation and evaluation tasks for nuclear reactor analysis. It was primarily created for fast reactor investigations, but later extended for thermal and epithermal reactor analysis of light water reactors.

5.2. Coupling method

The form of coupling which is used is a loose coupling. The source code of COBRA-TF and KARBUS are almost unchanged. The procedure *COBRAP.f* [Ref.XI] handles the coupling. Data transfer from KARBUS to COBRA is done by exchange of text files, which are generated after each run of the programs. The post-processing methods (see 5.3.1 and 5.3.2) are controlled by the subroutines *KCNTTI* and *KCTTNI* [Ref.XI].

KARBUS starts with a standard job and uses a restart option of KARBUS after the first iteration. This procedure permits to economize calculation time.

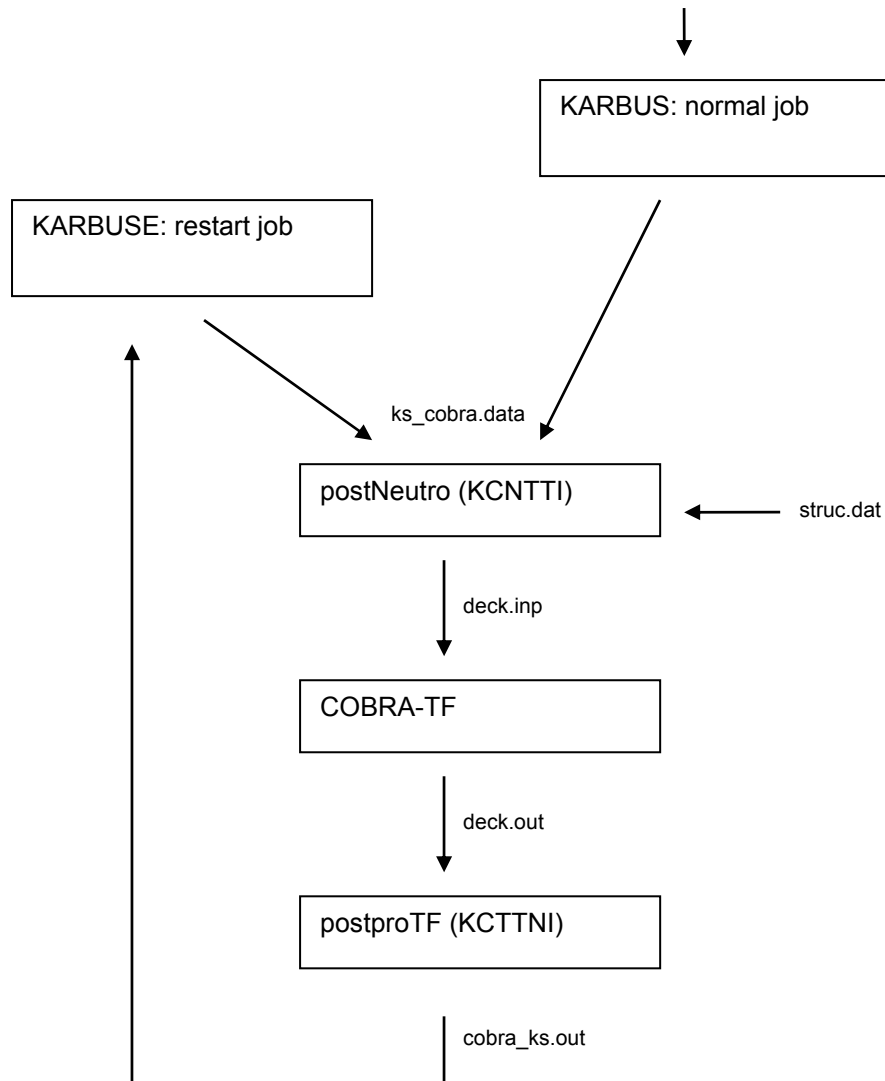


Figure 5-1: Coupling scheme

5.3. Post-processing of data

5.3.1. Post-processing of COBRA-TF output data

The COBRA-TF code returns output data in British units. Therefore, a conversion in SI units had to be performed. The water temperature is given for every channel, but an averaged value for every rod was needed. In addition, the coolant temperature data refers to junctions between two axial levels and not to the middle of a level. Clad and fuel temperatures refer to the middle of a level. The neutronic code demands average values for clad and pellet temperature values. The average value for the pellet temperature is calculated with the same method as COBRA-EN does.

For these tasks, the program *postproTF* in C++ was written. It consists of a function, which scans the COBRA-TF output file for the needed data, several other functions, which calculate average values and an output function, which writes the data file. This file contains the information assigned to 810

cells (10 levels x 81 rods). The neutronic code simulates a quarter of an assembly instead of an eight, containing 81 rods instead of 45. The cell numbering goes from the top to the bottom. Three arguments have to be transferred to the program:

- Input file: name of the data output of COBRA-TF (deck.out)
- Output file: target file for post-processed data (cobra_ks.out)
- Level: number of axial levels. The COBRA-TF output must be adapted to this number of levels.

5.3.2. Post-processing of KARBUS output data

The Neutronic code KARBUS writes an output file containing data assigned to the 810 cells mentioned before. The rod power has to be read, an average value calculated and this value and the relative rod power has to be inserted in a COBRA-TF input file. Therefore, an existing input file, containing all other information, has to be modified. An axial power profile is added for every rod.

The C++ program *postNeutro* fulfilling these tasks reads the KARBUS output file and the existing input file for COBRA-TF, modifies the average rod power value, and adds the power profile tables. Then it writes the new input file. Four arguments are transferred:

- Input file: name of output data file of KARBUS (ks_cobra.data)
- Output file: target file for post-processed data (deck.inp)
- Structure file: existing COBRA-TF input file, which is modified (struc.dat)
- Level: number of axial levels. The structure file must be adapted at this number of levels.

5.4. Transferring COBRA-TF from Windows to Linux

Both codes have to run on the same system to be able to couple KARBUS and COBRA-TF. COBRA-TF was usually used with Windows, while KARBUS only runs with Linux. Therefore, COBRA-TF had to be transferred to Linux. Three compilers, the Intel Fortran compiler *ifc*, the Lahey Fortran compiler *LF90* and the Portland compiler *pgi*, were available. Characterized with a standard simulation problem, the Windows, Lahey and Portland compiler show the same results. At this, the Lahey compiler only ran with the debug modus, so produced a program, which is very slow. To use the Portland compiler, the time controlling routine of the source code had to be changed. It was written for a windows system. The *ifc* compiler produced a program, which delivered data quickly with a 0.1% variation to the other compilers.

The original COBRA-TF source code includes a method to save output data in GRACE format *xdr*. This is packed in a windows library. In a first case, as no source code was available, the COBRA code was modified and the respective method calls were disabled. Later in a second case, a library for Linux was build. For this, the source code of plot program AcGrace (Analysis Code GRaphing, Advanced Computation and Exploration of data) was used, as it uses the same routines. [Ref.XII]

5.5. Results

A coupled job with 8 iteration was performed. The coupled codes required several days for the calculation, which is mainly caused by KARBUS since the COBRA-TF calculations required only 1 or 2 hours each.

A clear displacement of the power profile to the bottom of the rods is observable (Figure 5-2). This is due to the fact that on the bottom the water temperature is lower than at the outlet of the vessel. Therefore, its density is higher at the bottom. Neutrons perform more impacts with the moderator at this axial level. The thermalisation capability is stronger and as a consequence the rod power is higher. In addition, Figure 5-2 shows that the coupling needs some iterations before a stable power distribution is achieved.

Axial power distribution in PWR fuel assembly (GRS benchmark)

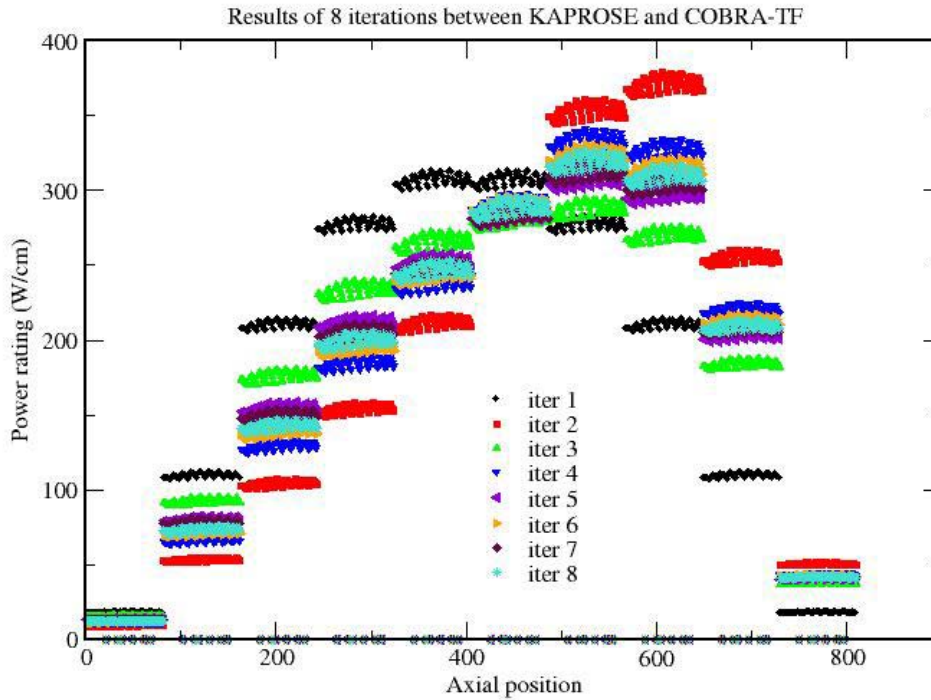


Figure 5-2 Coupling - Axial power distribution [Ref. XI]

(Axial position – node number from top to bottom)

A consequence of the displacement of the power rating is the changing of other characteristics like coolant temperature, density and fuel temperature. The fuel temperature shape is no more sinusoidal, but a displacement to the bottom is observable. Because of the stronger power rate at the bottom of the vessel the coolant is faster heated up. See Appendix G.

The shape of the power profile of a fuel rod is quite important since it affects directly the burn-up. That means that at positions with high power the fuel consumption is stronger than at positions with low power.

Chapter 6

CONCLUSION

For this study, several simulations with COBRA-EN and COBRA-TF were made. On the one hand, for each code an assembly simulation with open gaps and with closed gaps, on the other hand, core simulations with non- and radial dependent pin power were performed.

The procedure to undertake a COBRA-EN simulation is quite easy and fast. For this special problem, since it is steady state and non-boiling, COBRA-EN is an adequate tool.

COBRA-TF is more powerful. The fact that entrained droplets are considered is a strong improvement. The possibility to simulate the upper and lower plenum seems to be reasonable. Nevertheless, the creation of an input is difficult and an option for steady state solutions is clearly missing.

The obtained results for core simulations of both codes have the same order of magnitude. The differences, revealed by a difference in the outlet temperature, are caused by a pressure loss in the upper part of the active core in the COBRA-TF simulation. The results for the assembly simulations are less similar. For closed channels, the difference due to the pressure loss is noticed too. In addition, discrepancies for lower channels are observed. For open channels, the differences are huge. COBRA-EN and TF seems not to calculate the cross flow between subchannels the same way.

The coupling of COBRA-TF and KARBUS was realized under Linux. The importance of a coupling of thermo hydraulic and neutronic codes was demonstrated since a changing of the power rating, fuel and coolant temperature was observed.

The internship in the Institute for Reactor Safety of the FZK was quite interesting and instructive. It permitted a first approach to the work with up-to-date numerical simulation codes for nuclear engineering. Investigations in both fields, thermo hydraulic and neutronic, were made. Skills in FORTRAN and C++ coding were improved. The internship offered a look into the code structure of the COBRA codes and highlighted some difficulties in the handling of those simulation tools. A very careful and disciplined work method was indispensable for the creation of a COBRA-TF input file.

Working in a research institution was a good experience. It provided an insight into the day-to-day work environment of a scientist with its conferences, weekly seminars, and informal meetings. Every member of the department seems to be a specialist in his field, but they join to treat complex problems.

Chapter 7

PERSPECTIVES

Unfortunately, some improvements are still missing for satisfactory results. The COBRA-TF simulations should be revised. Taking into account of the upper and lower plenum seems to be reasonable after this work. A deeper look into the cross flow calculation with the turbulence mixing model is recommended.

For the coupling, separate axial subdivision for the thermo hydraulic code and the neutronic code should be considered. The data transferring programs should be able to interpolate between axial levels in order to allow for example 10 levels for the thermo hydraulic and 5 for the neutronic code. This would help to undertake quick, less precise, coupled calculations for testing.

In a next step, a direct coupling of the two codes is intended, i.e. the source code are modified and one code manage the second one. No transferring programs are needed.

Actually, the IRS proposes several student Master projects concerning the realized coupled code.

Appendix A EQUATIONS

COBRA-EN :

Mass Balance

The finite-difference equation for the conservation of mass can be written as:

$$A_i \frac{\Delta X_j}{\Delta t} (\rho_{ij} - \rho_{ij}^n) + m_{ij} - m_{ij-1} + \Delta X_j \sum_{k \in i} e_{ik} w_{kj} = 0 \quad (0.3)$$

where:

i	channel index
j	axial index
k	gap index
A	axial flow area (m ²)
ρ	$\alpha \rho_v + (1 - \alpha) \rho_l =$ mixture density (kg/m ³)
ρ^n	mixture density (kg/m ³) at the end of the previous time step (or at the beginning of the current one)
m	mixture axial mass flowrate (kg/s),
w	mixture crossflow rate (kg/m/s),
ρ_l	liquid density ($\rho_l = \rho_f$ for saturated liquid),
ρ_v	vapor density ($\rho_v = \rho_g$ for saturated vapor),
α	void fraction
e_{ik}	direction of crossflow

The first term is the actual mass in the control volume; the others specify the flow into the volume (flow from the bottom, flow to the top, crossflow).

Energy Balance

The conservation of energy can be written as:

$$\begin{aligned} & \frac{A_i}{\Delta t} \left[\rho_{ij}^n (h_{ij} - h_{ij}^n) + h_{ij} (\rho_{ij} - \rho_{ij}^n) \right] + \frac{1}{\Delta X_j} (m_{ij} h_{ij}^* - m_{ij-1} h_{ij-1}^*) + \sum_{k \in i} e_{ik} w_{kj} h_{kj}^* = \\ & = \sum_{r \in i} P_r \Phi_{ir} q''_{rj} - \sum_{k \in i} w'_{kj} (h_{ij} - h_{nj}) - \sum_{k \in i} C_k s_k (T_{ij} - T_{nj}) + \sum_{r \in i} I_Q \Phi_{ir} q'_{rj} \end{aligned} \quad (0.4)$$

where:

r	rod index
Φ_{ir}	fraction of rod r facing channel i
P_r	heated perimeter of rod r
h	$x h_v + (1 - x) h_l =$ mixture flowing enthalpy (J/kg)
h_n	enthalpy at the end of the previous time step
h_l	liquid enthalpy ($h_l = h_f$ for saturated liquid)
h_v	vapor enthalpy ($h_v = h_g$ for saturated vapor)
x	flowing steam quality
q''	heat flux from a fuel rod into the fluid, assumed uniform around the rod circumference (J/m ² /s)
q'	linear power generated in a rod (J/m/s),

w'	turbulent crossflow (J/m/s)
T	temperature (K)
n	$l+1-i$ = index of the channel adjacent to channel i through gap k ,
h_{ij}^*	flowing enthalpy (J/kg) at axial level j assumed as the donor cell enthalpy, i.e.,
	$h_{ij}^* = h_{ij} \quad \text{if } m_{ij} > 0$ $h_{ij}^* = h_{ij+1} \quad \text{if } m_{ij} < 0$
h_{kj}^*	flowing enthalpy (J/kg) for gap k assumed as the donor cell enthalpy, i.e.
	$h_{kj}^* = h_{ij} \quad \text{if } e_{ik} w_{kj} > 0$ $h_{kj}^* = h_{nj} \quad \text{if } e_{ik} w_{kj} < 0$
C_k	thermal conductance (J/s/m ² /K) in lateral directions
r_Q	fraction of the fission power generated in a fuel rod, that enters the coolant directly

On the left-hand side of the equation, energy storage (1st term) and flow into the control volume are defined. The 2nd term stands for axial flow and the 3rd term for crossflow. On the right-hand side, the 1st sum defines the heat flux from the fuel rod neighbored to channel i . The 2nd sum represents lateral energy exchange due to turbulent mixing and the 3rd sum lateral energy exchange due to conduction. The last sum stands for fission power, which is directly produced in the coolant of the channel.

The actual equation which is solved by the code is the continuity equation (0.5) multiplied by the flowing enthalpy h_{ij} and subtracted by the energy equation (0.6).

Momentum Balance

The model for the momentum balance is divided into the axial momentum balance equation (0.7) and the lateral momentum balance equation (0.8).

The first balance equation can be written as:

$$\frac{\Delta X_j}{\Delta t} (m_{ij} - m_{ij}^n) + m_{ij} U'_{ij} - m_{ij-1} U'_{ij} + \Delta X_j \sum_{k \in i} e_{ik} w_{kj} U'_{kj}^* =$$

$$- A_i (P_{ij} - P_{i-1}) - g A_i \Delta X_j \rho_j \cos \theta - \frac{1}{2} \left(\frac{\Delta X f \phi^2}{D_h \rho_l} + K v^* \right) \left| \frac{m_{ij}}{A_i} \right| - f_T \Delta X_j \sum_{k \in i} w'_{kj} (U'_{ij} - U'_{nj}) \quad (0.5)$$

with:

g	gravity acceleration
P	pressure (N/m ²),
θ	inclination of the channels with respect to the vertical
f	friction factor
ϕ^2	two-phase friction multiplier
K	pressure loss coefficient for grid spacers or grid plates
f_T	transverse momentum factor
v'	effective specific volume for momentum transport with
	$v' = \frac{x^2}{\alpha \rho_v} + \frac{(1-x)^2}{(1-\alpha) \rho_l}$
U'	related effective momentum velocity:
	$U' = \frac{m}{A} v'^*$

The left-hand side of the momentum balance equation defines the storage, the flow in axial direction and the crossflow. The right-hand side represents the impact of axial pressure difference (1st term), vertical component of fluid weight (2nd term), pressure loss by wall friction and other elements (3rd term) are represented. The last term stands for lateral momentum exchange due to turbulent mixing.

The lateral momentum equation can be written as:

$$\frac{\Delta X_j}{\Delta t} (w_{kj} - w_{kj}^n) + \bar{U}'_{kj} w_{kj}^* - \bar{U}'_{kj-1} w_{kj-1}^* = \frac{S_k}{l_k} \Delta X_j P_{kj-1} - \frac{1}{2} \left(K_G \frac{\Delta X v^*}{sl} \right)_{kj} |w_{kj}| w_{kj} \quad (0.6)$$

with:

\bar{U}'_{kj} = the momentum velocity for a gap is the arithmetic mean of the momentum velocity of the channels connected by the gap

P_{kj-1} = $P_{|j-1} - P_{|j}$ - pressure difference between two cells

K_G = loss coefficient

S = gap width

and

$$w_{kj}^* = w_{kj} \quad \text{if } \bar{U}'_{kj} > 0$$

$$w_{kj}^* = w_{kj+1} \quad \text{if } \bar{U}'_{kj} < 0$$

The left part of the equation deals with the storage of momentum and the flow in axial direction. The right part consists of two terms due to lateral pressure difference and the loss of pressure caused by flow through the gap.

Heat Transfer Coefficient

The heat transfer coefficient of the liquid phase forced convection is calculated by:

$$H_{D-B,l} = 0.023 \frac{k_l}{D_H} \left(\frac{G_l D_H}{\mu_l} \right)^{0.8} (Pr_l)^{0.4} \quad (0.7)$$

where

$$\frac{G_l D_H}{\mu_l} = Re \quad (0.8)$$

with:

k	thermal conductivity
D_H	hydraulic Diameter
G	mass flux
μ	viscosity
Pr	Prandtl number

And the heat transfer for nucleate boiling with the Thom correlation (see [Ref.xiii]):

$$H_{T_{\text{hom}}} = \left[e^{P/1260} \cdot (T_w - T_{\text{sat}}) / 0.072 \right]^2 / (T_w - T_b) \quad (0.9)$$

with

P	system pressure (psia)
T_w	wall temperature (°F)
T_{sat}	fluid saturation temperature (°F)
T_b	fluid temperature

The heat transfer in this region consists of a part liquid-forced convection and another part Thom heat transfer.

COBRA-TF:

Heat transfer correlations

Dittus-Boelter correlation for steam:

$$H_{D-B,v} = 0.023 \frac{k_V}{D_H} \left(\frac{G_V D_H}{\mu_V} \right)^{0.8} (\text{Pr}_V)^{0.4} \quad (0.10)$$

Laminar flow correlation:

$$H_{\text{lam}} = 7.86 \frac{k_l}{D_H} \quad (0.11)$$

Appendix C

COBRA-EN FIGURES

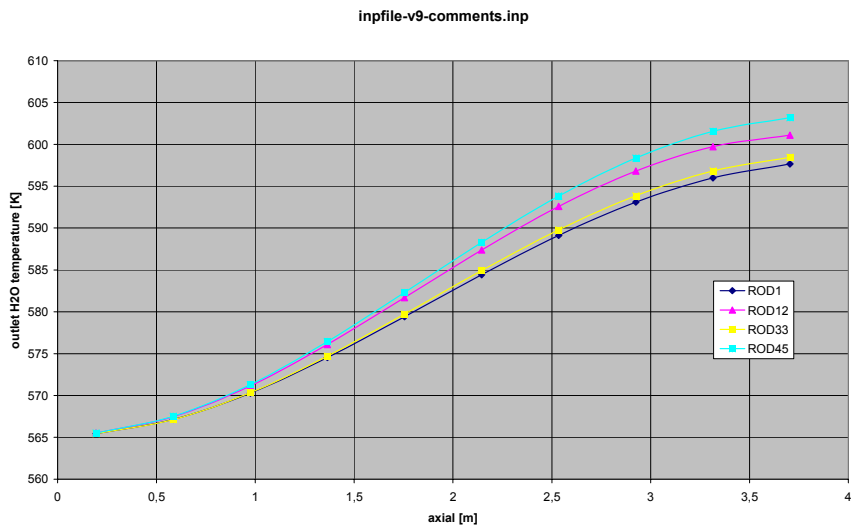


Figure C-1: COBRA-EN assembly simulation with crossflow - coolant temperature

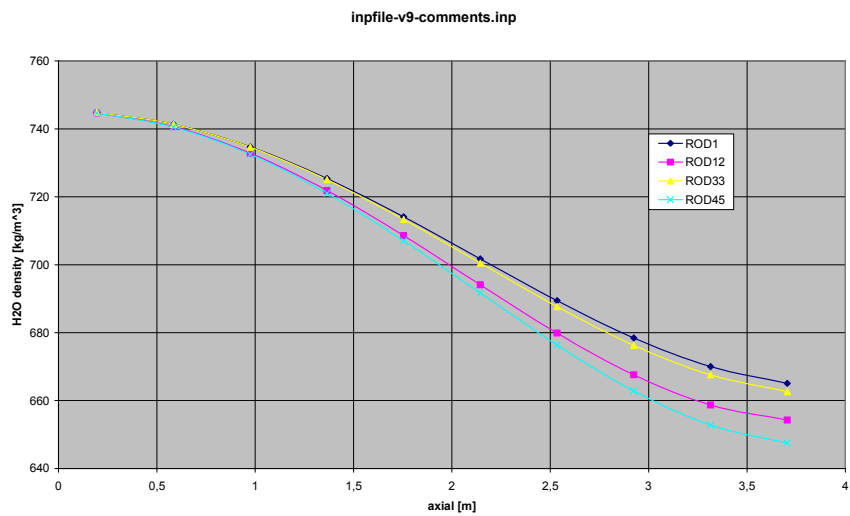


Figure C-2: COBRA-EN assembly simulation with crossflow - coolant density

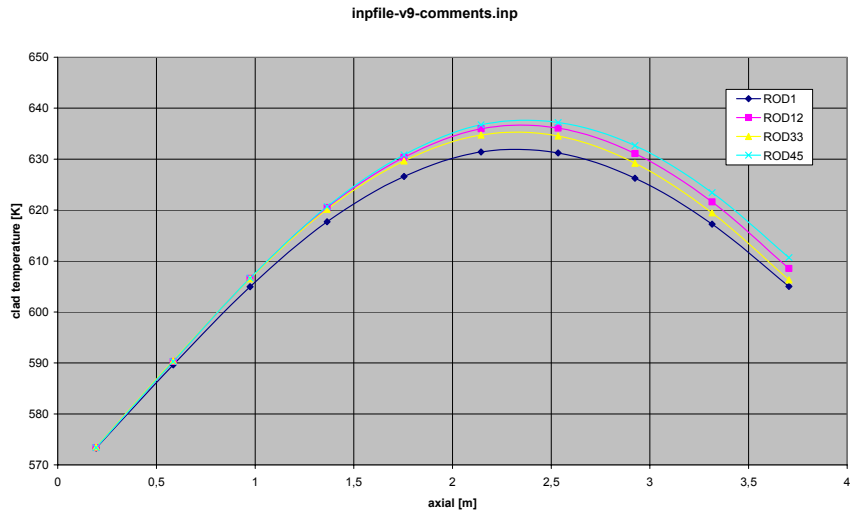


Figure C-3: COBRA-EN assembly simulation with crossflow - clad temperature

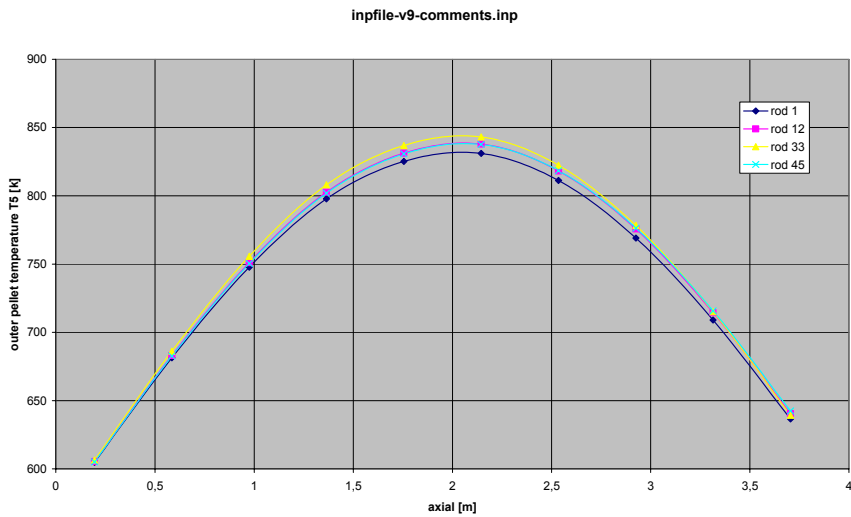


Figure C-4: COBRA-EN assembly simulation with crossflow - outer pellet temperature

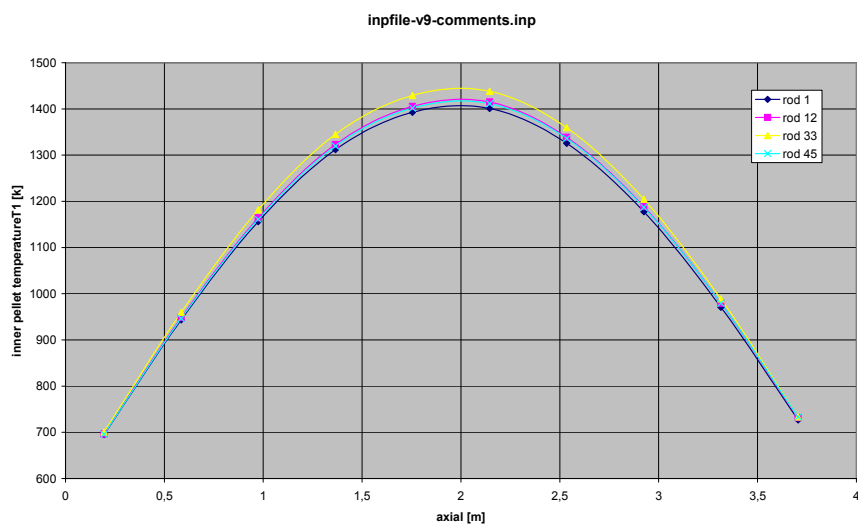


Figure C-5: COBRA-EN assembly simulation with crossflow - inner pellet temperature

Appendix D

HEADER FILE “RESPAR.H”

Changes to the version from 1999 that were made are declared with *cchecker*.

```

c *****
c last delta @#respar.h
c created on 03/15/94
c current date 07/12/1999
c Large Problems
c *****
c
cchecker: adaptation to PWR18x18-14
cchecker 55 subchan. and 45 rods
c
c
c -----
c turbulence flag - 1 on, 0 off:
integer,parameter,private :: iftrb=0
c
c -----
c max number of channels in one section
cchecker integer,parameter,private :: mbdim=50
integer,parameter,private :: mbdim=60
c
c -----
c total number of channels:
integer,parameter,private :: mcdim=100
c
c -----
c Number of records read for transverse orthogonal
momentum
c convection:
integer,parameter,private :: mddim=300
c
c -----
c Number of fuel geom types:
integer,parameter,private :: mfdim=10
c
c -----
c Number of transverse connections:
cchecker integer,parameter,private :: mgdim=100
integer,parameter,private :: mgdim=300
c
c -----
c Number of components dumped for graphics ???:
integer,parameter,private :: mhdim=20
c
c -----
c Number of graphics dumps to be made:
c allocated integer,parameter,private :: midim=300
c
c -----
c Number of spacer grid types:
integer,parameter,private :: mjdim=4
c
c -----
c Maximum number of axial locations times the number
of
c channels having the same grid type:
integer,parameter,private :: mkdim=300
c
c -----
c Number of vertical variation tables:
integer,parameter,private :: mldim=5
c
c -----
c Number of flow blockages:
integer,parameter,private :: mndim=1
c
c -----
c Number of rods:
cchecker integer,parameter,private :: mrdim=30
integer,parameter,private :: mrdim=60
c
c -----
c Number of pressure or flow boundary conditions:
cchecker integer,parameter,private :: msdim=30
integer,parameter,private :: msdim=120
c
c -----
c Number of material property types:
integer,parameter,private :: mtdim=10
c
c -----
c Number of vertical boundary conditions:
cchecker integer,parameter,private :: mudim=30
integer,parameter,private :: mudim=140
c
c -----
c Number of forcing functions for boundary conditions:
integer,parameter,private :: mvdim=10
c
c -----
c Number of vertical nodes in one section:
cchecker integer,parameter,private :: mxdim=300
integer,parameter,private :: mxdim=800
c
c -----
c Maximum value of NAMGAP+1 in card group 2:
integer,parameter,private :: mydim=20
c
c -----
c Number of continuity cells:
cchecker integer,parameter,private :: nadim=300
integer,parameter,private :: nadim=1500
c
c -----
c Number of flow connections to a cell:
integer,parameter,private :: nbdim=30
c
c -----
c Bandwidth of pressure solution matrix:
cchecker integer,parameter,private :: nedim=100
integer,parameter,private :: nedim=300
c
c -----
c Maximum number of data pairs in forcing function
tables:
integer,parameter,private :: nfdim=50
c
c -----
c Maximum number of cells in any one simultaneous
solution group:
cchecker integer,parameter,private :: nidim=300
integer,parameter,private :: nidim=1500
c
c -----
c Number of transverse momentum cells that have flow
set to zero:
integer,parameter,private :: nldim=1
c
c -----
c Number of gas species in noncondensable gas
mixture:
integer,parameter,private :: nmdim=2
c
c -----

```

```

c -----
c Number of radial nodes in heated conductors:
integer,parameter,private :: nndim=20
c -----
c -----
c Number of entries in a material property table:
integer,parameter,private :: npdim=20
c -----
c -----
c Number of sections:
integer,parameter,private :: nqdim=20
c -----
c -----
c Total number of heated conductor segments:
cchecker integer,parameter,private :: nrdim=40
integer,parameter,private :: nrdim=200
c -----
c -----
c Number of radiation channels
integer,parameter,private :: nsdim=20
c -----
c -----
c Number of unheated conductors:
integer,parameter,private :: ntdim=10
c -----
c -----
c Number of azimuthal heat transfer segments in heated
conductors:
cchecker integer,parameter,private :: nudim=50
integer,parameter,private :: nudim=300
c -----
c -----
c Number of radiation channel location types:
integer,parameter,private :: nwdim=10
c -----
c -----
c Number of vertical nodes in heated conductors:
cchecker integer,parameter,private :: nxdim=300
integer,parameter,private :: nxdim=600

```

```

c -----
c -----
c Number of radial nodes + 2 in unheated conductor:
integer,parameter,private :: nydim=10
c -----
c -----
c Number of vertical levels in mesh all sections:
cchecker integer,parameter,private :: nzdim=300
integer,parameter,private :: nzdim=600
c -----
c -----
c Maximum of nndim and nydim:
integer,parameter,private :: n1dim=20
c -----
c -----
c Number of axial power profile tables:
cchecker integer,parameter,private :: n3dim=5
integer,parameter,private :: n3dim=50
c -----
c -----
c Number of thermal conductor temperature initialization
tables:
integer,parameter,private :: n4dim=5
c -----
c -----
c Maximum number of entries in temperature
initialization tables:
cchecker integer,parameter,private :: n5dim=10
integer,parameter,private :: n5dim=50
c -----
c -----
c max[mxdim,nxdim]+2:
integer,parameter,private :: n7dim=802
c -----
c -----
c Number of nuclear fuel rods using dynamic gap
conductance model:
integer,parameter,private :: n8dim=5
c -----

```

Appendix E

COBRA-TF INPUT FILE FOR AN ASSEMBLY ANALYSIS

COBRA-TF input file: *deck-ch55-sinPw-rad-all-v4.inp*

As the input file is too long for this Appendix, repetitive parts are skipped with (...).

```

*****
* INPUT DECK *
*
* Sub-Channel model - PWR18x18-24_fa_model.inp
* -55 subchannels + 45 rods;
* -sin-Power; radial dependency; rods 10,21,24,33 zeroPw *
* -90 gaps with transverse and ortho. connection
* -> steady state after 5 sec.
*material properties changed! (values from cobraEN manual)
*
* by BECKER, Björn          IRS, FZK July 2005
*
*****
*
* ICOBRA
* 1
* DTSTEP  TIMET
* 0 0.0
* EPSO  OITMAX  IITMAX
* .005  20  40
* INIT
* 1  ***1." Sub-Channel Model of PWR18x18-24 Bundle *****
*
*****
*GROUP 1 - Calculation Variables and Initial Conditions *
*****
*NGRP NGAS
* 1 1
* PREF  HIN  GIN  AFLUX  GHIN  VFRAC1  VFRAC2  RSBF
* .276E6 2.720E6  0 17.04973 1.56E6 .0000 .9999 1.0
* 15.8E6 2.591E6  0 17.04973 1.56E6 1.0000 .9999 1.0
*GTYPE  VFRAC
air  .0001
*
*****
*GROUP 2 - Channel Description *
*****
*NGRP NCHA
* 2 55
* 1 AN PW ABOT ATOP NMGP
* 116E-638E-4 0.0 0.0 2
*INOD KGPB KGPA INOD KGPB KGPA
* 11 1 0 1 0 1
* 1 AN PW ABOT ATOP NMGP
* 254E-615E-3 0.0 0.0 6
*INOD KGPB KGPA INOD KGPB KGPA INOD KGPB KGPA INOD KGPB KGPA
* 11 1 0 11 2 0 11 3 0 1 0 1 1 0 2
* 1 0 3
* 1 AN PW ABOT ATOP NMGP
* 345E-615E-3 0.0 0.0 4
*INOD KGPB KGPA INOD KGPB KGPA
* 11 2 0 11 4 0 1 0 2 1 0 4
* 1 AN PW ABOT ATOP NMGP
* 454E-615E-3 0.0 0.0 6
*INOD KGPB KGPA INOD KGPB KGPA INOD KGPB KGPA INOD KGPB KGPA INOD KGPB KGPA
* 11 3 0 11 5 0 11 7 0 1 0 3 1 0 5
* 1 0 7
* 1 AN PW ABOT ATOP NMGP
* 590E-630E-3 0.0 0.0 8
*INOD KGPB KGPA INOD KGPB KGPA INOD KGPB KGPA INOD KGPB KGPA INOD KGPB KGPA
* 11 4 0 11 5 0 11 6 0 11 8 0 1 0 4
* 1 0 5 1 0 6 1 0 8
* 1 AN PW ABOT ATOP NMGP
* 645E-615E-3 0.0 0.0 4

```

```

*INOD KGPB KGPA INOD KGPB KGPA INOD KGPB KGPA INOD KGPB KGPA
  11 6 0 11 9 0 1 0 6 1 0 9
* I AN PW ABOT ATOP NMGP
  754E-615E-3 0.0 0.0 6
*INOD KGPB KGPA INOD KGPB KGPA INOD KGPB KGPA INOD KGPB KGPA INOD KGPB KGPA
  11 7 0 11 10 0 11 13 0 1 0 7 1 0 10
  1 0 13
* I AN PW ABOT ATOP NMGP
  890E-630E-3 0.0 0.0 8
*INOD KGPB KGPA INOD KGPB KGPA INOD KGPB KGPA INOD KGPB KGPA INOD KGPB KGPA
  11 8 0 11 10 0 11 11 0 11 14 0 1 0 8
  1 0 10 1 0 11 1 0 14
* I AN PW ABOT ATOP NMGP
  990E-630E-3 0.0 0.0 8
*INOD KGPB KGPA INOD KGPB KGPA INOD KGPB KGPA INOD KGPB KGPA INOD KGPB KGPA
  11 9 0 11 11 0 11 12 0 11 15 0 1 0 9
  1 0 11 1 0 12 1 0 15
* I AN PW ABOT ATOP NMGP
  1045E-615E-3 0.0 0.0 4
*INOD KGPB KGPA INOD KGPB KGPA INOD KGPB KGPA INOD KGPB KGPA INOD KGPB KGPA
  11 12 0 11 16 0 1 0 12 1 0 16
* I AN PW ABOT ATOP NMGP
  1154E-615E-3 0.0 0.0 6
*INOD KGPB KGPA INOD KGPB KGPA INOD KGPB KGPA INOD KGPB KGPA INOD KGPB KGPA
  11 13 0 11 17 0 11 21 0 1 0 13 1 0 17
  1 0 21
* I AN PW ABOT ATOP NMGP
  1290E-630E-3 0.0 0.0 8
*INOD KGPB KGPA INOD KGPB KGPA INOD KGPB KGPA INOD KGPB KGPA INOD KGPB KGPA
  11 14 0 11 17 0 11 18 0 11 22 0 1 0 14
  1 0 17 1 0 18 1 0 22
* I AN PW ABOT ATOP NMGP
  1390E-630E-3 0.0 0.0 8
*INOD KGPB KGPA INOD KGPB KGPA INOD KGPB KGPA INOD KGPB KGPA INOD KGPB KGPA
  11 15 0 11 18 0 11 19 0 11 23 0 1 0 15
  1 0 18 1 0 19 1 0 23

```

(...)

```

* I AN PW ABOT ATOP NMGP
  5045E-615E-3 0.0 0.0 6
*INOD KGPB KGPA INOD KGPB KGPA INOD KGPB KGPA INOD KGPB KGPA INOD KGPB KGPA
  11 77 0 11 85 0 11 86 0 1 0 77 1 0 85
  1 0 86
* I AN PW ABOT ATOP NMGP
  5145E-615E-3 0.0 0.0 6
*INOD KGPB KGPA INOD KGPB KGPA INOD KGPB KGPA INOD KGPB KGPA INOD KGPB KGPA
  11 78 0 11 86 0 11 87 0 1 0 78 1 0 86
  1 0 87
* I AN PW ABOT ATOP NMGP
  5245E-615E-3 0.0 0.0 6
*INOD KGPB KGPA INOD KGPB KGPA INOD KGPB KGPA INOD KGPB KGPA INOD KGPB KGPA
  11 79 0 11 87 0 11 88 0 1 0 79 1 0 87
  1 0 88
* I AN PW ABOT ATOP NMGP
  5345E-615E-3 0.0 0.0 6
*INOD KGPB KGPA INOD KGPB KGPA INOD KGPB KGPA INOD KGPB KGPA INOD KGPB KGPA
  11 80 0 11 88 0 11 89 0 1 0 80 1 0 88
  1 0 89
* I AN PW ABOT ATOP NMGP
  5445E-615E-3 0.0 0.0 6
*INOD KGPB KGPA INOD KGPB KGPA INOD KGPB KGPA INOD KGPB KGPA INOD KGPB KGPA
  11 81 0 11 89 0 11 90 0 1 0 81 1 0 89
  1 0 90
* I AN PW ABOT ATOP NMGP
  5511E-637E-4 0.0 0.0 2
*INOD KGPB KGPA INOD KGPB KGPA
  11 90 0 1 0 90

```

```

*****
* GROUP 3 - Transverse Channel Connection (Gap) Data *
*****

```

```

*NGRP NK
  3 90
* K IK JK GAPN LNGT WKR FWAL IGPB IGPA FACT IGAP JGAP
  1 1 2.0023.0099 0.5 0.0 0 0 1.0 0 3

```


*GMLT ETNR
1. 0.0
* K IK JK GAPN LNGT WKR FWAL IGPB IGPA FACT IGAP JGAP
2 2 3.0032.0099 0.5 0.0 0 0 1.0 0 4
*GMLT ETNR
1. 0.0
* K IK JK GAPN LNGT WKR FWAL IGPB IGPA FACT IGAP JGAP
3 2 4.0023.0127 0.5 0.0 0 0 1.0 1 7
*GMLT ETNR
1. 0.0
* K IK JK GAPN LNGT WKR FWAL IGPB IGPA FACT IGAP JGAP
4 3 5.0032.0127 0.5 0.0 0 0 1.0 2 8
*GMLT ETNR
1. 0.0
* K IK JK GAPN LNGT WKR FWAL IGPB IGPA FACT IGAP JGAP
5 4 5.0032.0099 0.5 0.0 0 0 1.0 0 6
*GMLT ETNR
1. 0.0
* K IK JK GAPN LNGT WKR FWAL IGPB IGPA FACT IGAP JGAP
6 5 6.0032.0127 0.5 0.0 0 0 1.0 5 9
*GMLT ETNR
1. 0.0
* K IK JK GAPN LNGT WKR FWAL IGPB IGPA FACT IGAP JGAP
7 4 7.0023.0127 0.5 0.0 0 0 1.0 3 13
*GMLT ETNR
1. 0.0
* K IK JK GAPN LNGT WKR FWAL IGPB IGPA FACT IGAP JGAP
8 5 8.0032.0127 0.5 0.0 0 0 1.0 4 14
*GMLT ETNR
1. 0.0
* K IK JK GAPN LNGT WKR FWAL IGPB IGPA FACT IGAP JGAP
9 6 9.0032.0127 0.5 0.0 0 0 1.0 6 15
*GMLT ETNR
1. 0.0
* K IK JK GAPN LNGT WKR FWAL IGPB IGPA FACT IGAP JGAP
10 7 8.0032.0099 0.5 0.0 0 0 1.0 0 11
*GMLT ETNR
1. 0.0
* K IK JK GAPN LNGT WKR FWAL IGPB IGPA FACT IGAP JGAP
11 8 9.0032.0127 0.5 0.0 0 0 1.0 10 12
*GMLT ETNR
1. 0.0
* K IK JK GAPN LNGT WKR FWAL IGPB IGPA FACT IGAP JGAP
12 9 10.0032.0127 0.5 0.0 0 0 1.0 11 16
*GMLT ETNR
1. 0.0

(...)

* K IK JK GAPN LNGT WKR FWAL IGPB IGPA FACT IGAP JGAP
80 44 53.0032.0095 0.5 0.0 0 0 1.0 64 0
*GMLT ETNR
1. 0.0
* K IK JK GAPN LNGT WKR FWAL IGPB IGPA FACT IGAP JGAP
81 45 54.0032.0127 0.5 0.0 0 0 1.0 72 0
*GMLT ETNR
1. 0.0
* K IK JK GAPN LNGT WKR FWAL IGPB IGPA FACT IGAP JGAP
82 46 47.0016.0099 0.5 0.0 0 0 1.0 0 83
*GMLT ETNR
1. 0.0
* K IK JK GAPN LNGT WKR FWAL IGPB IGPA FACT IGAP JGAP
83 47 48.0016.0127 0.5 0.0 0 0 1.0 82 84
*GMLT ETNR
1. 0.0
* K IK JK GAPN LNGT WKR FWAL IGPB IGPA FACT IGAP JGAP
84 48 49.0016.0127 0.5 0.0 0 0 1.0 83 85
*GMLT ETNR
1. 0.0
* K IK JK GAPN LNGT WKR FWAL IGPB IGPA FACT IGAP JGAP
85 49 50.0016.0127 0.5 0.0 0 0 1.0 84 86
*GMLT ETNR
1. 0.0
* K IK JK GAPN LNGT WKR FWAL IGPB IGPA FACT IGAP JGAP
86 50 51.0016.0127 0.5 0.0 0 0 1.0 85 87

```

*GMLT ETNR
1. 0.0
* K IK JK GAPN LNGT WKR FWAL IGPB IGPA FACT IGAP JGAP
87 51 52.0016.0127 0.5 0.0 0 0 1.0 86 88
*GMLT ETNR
1. 0.0
* K IK JK GAPN LNGT WKR FWAL IGPB IGPA FACT IGAP JGAP
88 52 53.0016.0127 0.5 0.0 0 0 1.0 87 89
*GMLT ETNR
1. 0.0
* K IK JK GAPN LNGT WKR FWAL IGPB IGPA FACT IGAP JGAP
89 53 54.0016.0127 0.5 0.0 0 0 1.0 88 90
*GMLT ETNR
1. 0.0
* K IK JK GAPN LNGT WKR FWAL IGPB IGPA FACT IGAP JGAP
90 54 55.0016.0095 0.5 0.0 0 0 1.0 89 0
*GMLT ETNR
1. 0.0
*NLGP
162
*KGP1 KGP2 KGP3 KGP1 KGP2 KGP3 KGP1 KGP2 KGP3 KGP1 KGP2 KGP3
1 2 1 2 2 1 2 4 3 3 5 2
4 5 2 4 6 4 5 4 3 5 8 7
6 6 4 6 9 8 7 10 5 8 10 5
8 11 6 9 11 6 9 12 9 10 8 7
10 14 13 11 9 8 11 15 14 12 12 9
12 16 15 13 17 10 14 17 10 14 18 11
15 18 11 15 19 12 16 20 16 17 14 13
17 22 21 18 15 14 18 23 22 19 16 15
19 24 23 20 20 16 20 25 24 21 26 17
22 26 17 22 27 18 23 27 18 23 28 19
24 28 19 24 29 20 25 29 20 25 30 25
26 22 21 26 32 31 27 23 22 27 33 32
28 24 23 28 34 33 29 25 24 29 35 34
30 30 25 30 36 35 31 37 26 32 37 26
32 38 27 33 38 27 33 39 28 34 39 28
34 40 29 35 40 29 35 41 30 36 41 30
36 42 36 37 32 31 37 44 43 38 33 32
38 45 44 39 34 33 39 46 45 40 35 34
40 47 46 41 36 35 41 48 47 42 42 36
42 49 48 43 50 37 44 50 37 44 51 38
45 51 38 45 52 39 46 52 39 46 53 40
47 53 40 47 54 41 48 54 41 48 55 42
49 55 42 49 56 49 50 44 43 50 58 57
51 45 44 51 59 58 52 46 45 52 60 59
53 47 46 53 61 60 54 48 47 54 62 61
55 49 48 55 63 62 56 56 49 56 64 63
57 65 50 58 65 50 58 66 51 59 66 51
59 67 52 60 67 52 60 68 53 61 68 53
61 69 54 62 69 54 62 70 55 63 70 55
63 71 56 64 71 56 64 72 64 65 58 57
65 74 73 66 59 58 66 75 74 67 60 59
67 76 75 68 61 60 68 77 76 69 62 61
69 78 77 70 63 62 70 79 78 71 64 63
71 80 79 72 72 64 72 81 80 73 82 65
74 82 65 74 83 66 75 83 66 75 84 67
76 84 67 76 85 68 77 85 68 77 86 69
78 86 69 78 87 70 79 87 70 79 88 71
80 88 71 80 89 72 81 89 72 81 90 81
82 74 73 83 75 74 84 76 75 85 77 76
86 78 77 87 79 78 88 80 79 89 81 80
90 90 81 16 19 12
*****
* GROUP 4 - Vertical Channel Connection Data *
*****
*NGRP NSEC NSIM IREB
4 1 3 1
*ISEC NCHN NONO DXS IVAR
1 55 10 .390 0
* I KCHA KCHA KCHA KCHA KCHA KCHA KCHB KCHB KCHB KCHB KCHB KCHB
1 1 1
2 2 2
3 3 3
4 4 4
5 5 5

```

(...)

```

50 50          50
51 51          51
52 52          52
53 53          53
54 54          54
55 55          55

```

```

*IWDE
100
*MSIM
100 210 550
*

```

```

*****
*GROUP 7 - Local Loss Coefficient and Grid Spacer Data *
*****

```

```

*NGRP NCD NGT IFGQ IFSD IFES IFTP NFBS
* 7 0 0 0 0 0 0 0 0 0 0
*

```

```

*****
* GROUP 8 - Rod and Unheated Conductor Data *
*****

```

```

*NGRP NRRD NSRD NC NRTB NRAD NLTY NSTA NXF NCAN RADF
8 45 0 1 3 0 0 0 1 0 0
* NIFTY IAXP NRND DAXMIN RMULT RADIAL HGAP ISEC HTMB TAMB
1 1 1 1 13E-4 1. 0.9801 5670. 1 0.
*NSCH PIE NSCH PIE NSCH PIE
1.125 2 .25 3.125
* NIFTY IAXP NRND DAXMIN RMULT RADIAL HGAP ISEC HTMB TAMB
2 1 1 1 13E-4 1. 0.9819 5670. 1 0.
*NSCH PIE NSCH PIE NSCH PIE NSCH PIE
2.25 3 .25 4 .25 5 .25
* NIFTY IAXP NRND DAXMIN RMULT RADIAL HGAP ISEC HTMB TAMB
3 1 1 1 13E-4 1. 0.9829 5670. 1 0.
*NSCH PIE NSCH PIE NSCH PIE
3.125 5 .25 6.125
* NIFTY IAXP NRND DAXMIN RMULT RADIAL HGAP ISEC HTMB TAMB
4 1 1 1 13E-4 1. 0.9830 5670. 1 0.
*NSCH PIE NSCH PIE NSCH PIE NSCH PIE
4.25 5 .25 7 .25 8 .25
* NIFTY IAXP NRND DAXMIN RMULT RADIAL HGAP ISEC HTMB TAMB
5 1 1 1 13E-4 1. 0.9859 5670. 1 0.
*NSCH PIE NSCH PIE NSCH PIE NSCH PIE
5.25 6 .25 8 .25 9 .25
* NIFTY IAXP NRND DAXMIN RMULT RADIAL HGAP ISEC HTMB TAMB
6 1 1 1 13E-4 1. 0.9941 5670. 1 0.
*NSCH PIE NSCH PIE NSCH PIE NSCH PIE
6.125 9 .25 10.125

```

(...)

```

* NIFTY IAXP NRND DAXMIN RMULT RADIAL HGAP ISEC HTMB TAMB
42 1 1 1 13E-4 1. 1.0048 5670. 1 0.
*NSCH PIE NSCH PIE NSCH PIE NSCH PIE
42.25 43 .25 51 .25 52 .25
* NIFTY IAXP NRND DAXMIN RMULT RADIAL HGAP ISEC HTMB TAMB
43 1 1 1 13E-4 1. 0.9943 5670. 1 0.
*NSCH PIE NSCH PIE NSCH PIE NSCH PIE
43.25 44 .25 52 .25 53 .25
* NIFTY IAXP NRND DAXMIN RMULT RADIAL HGAP ISEC HTMB TAMB
44 1 1 1 13E-4 1. 0.9904 5670. 1 0.
*NSCH PIE NSCH PIE NSCH PIE NSCH PIE
44.25 45 .25 53 .25 54 .25
* NIFTY IAXP NRND DAXMIN RMULT RADIAL HGAP ISEC HTMB TAMB
45 1 1 1 13E-4 1. 0.9863 5670. 1 0.
*NSCH PIE NSCH PIE NSCH PIE NSCH PIE
45.125 54 .25 55.125
* INRT1 NST1 NRX1
1 20 0 5
*IRTB IRTB IRTB IRTB IRTB IRTB IRTB IRTB IRTB IRTB IRTB
1 2 3 4 5 6 7 8 9 10 11 12
13 14 15 16 17 18 19 20
*****

```

* Initial heater rod temperature profile *

```

*****
* AXIALT TRINIT AXIALT TRINIT AXIALT TRINIT AXIALT TRINIT
  0.0 580.0 1.00 600.0 2.00 700.0 3.00 600.0
  3.9 580.0
*
* I NRT1 NST1 NRX1
  2 20 0 5
*IRTB IRTB IRTB IRTB IRTB IRTB IRTB IRTB IRTB IRTB IRTB IRTB
  21 22 23 24 25 26 27 28 29 30 31 32
  33 34 35 36 37 38 39 40
*****
* Initial heater rod temperature profile *
*****
* AXIALT TRINIT AXIALT TRINIT AXIALT TRINIT AXIALT TRINIT
  0.0 580.0 1.00 600.0 2.00 700.0 3.00 600.0
  3.9 580.0
*
* I NRT1 NST1 NRX1
  3 5 0 5
*IRTB IRTB IRTB IRTB IRTB IRTB IRTB IRTB IRTB IRTB IRTB
  41 42 43 44 45
*****
* Initial heater rod temperature profile *
*****
* AXIALT TRINIT AXIALT TRINIT AXIALT TRINIT AXIALT TRINIT
  0.0 580.0 1.00 600.0 2.00 700.0 3.00 600.0
  3.9 580.0
*
*****
* GROUP 9 - Conductor Geometry Description *
*****
*NGRP NFLT IREF ICOF IMWR
  9 1 0 0 0
* I FTYP DROD DFUL NFUL IMAC IMTX IMAX DCRE TCLD FTDS IGPC IGFC IRAP
  1 nucl .0095 .00805 5 1 2 2 064E-5 1 0 0 0
*
*****
* GROUP 10 - Material Properties *
*****
*NGRP NMAT
  10 2
* N NTDP RCOLD IMATAN
  1 2 10970. UO2
* TPROP CPF1 THCF TPROP CPF1 THCF
  200. 242.672 3.46 2000. 242.672 3.46
* N NTDP RCOLD IMATAN
  2 2 6552. zirconium
* TPROP CPF1 THCF TPROP CPF1 THCF
  200. 242.67 15.22 2000. 242.67 15.22
*
*****
*GROUP 11 - Axial Power Tables and Forcing Functions *
*****
*NGRP NAXP NQ NGPF
  11 1 4 0
* I NAXN
  1 12
* Y AXIAL Y AXIAL Y AXIAL Y AXIAL
  0.0 0.0 0.2 0.24 0.59 0.71 0.98 1.11
  1.37 1.39 1.76 1.55 2.15 1.55 2.54 1.39
  2.93 1.11 3.32 0.71 3.71 0.24 3.90 0.0
*
* YQ FQ YQ FQ YQ FQ YQ FQ
*
  0.0 0.0 1.0 0.0 2.0 1.0 500.0 1.0
*
*****
*GROUP 12 - Turbulent Mixing Data *
*****
*NGRP N1
  12 1
* I BETA AAK
  1 0.01 1.0
*
*****
* GROUP 13 - Boundary Condition Data *
*****

```

```

*NGRP NBND NKBD NFUN NGBD
 13 110 0 2 0 0
*NPTS
 3 3
*ABSC ORDINT ABSC ORDINT ABSC ORDINT
 0.0 0.0 0.01 1.01500. 1.0
 0.0 0.1 0.2 1.01500. 1.0
*IBD1 IBD2 ISPC NPFN NHFN PVALUE HVALUE XVALUE
 1 1 2 1 25.1710E-02 1.295E6 15.87E6
*HMGA GVAL
1.6E6 1.0.9999.0001

*IBD1 IBD2 ISPC NPFN NHFN PVALUE HVALUE XVALUE
 2 1 2 1 21.7492E-01 1.295E6 15.87E6
*HMGA GVAL
1.6E6 1.0.9999.0001

*IBD1 IBD2 ISPC NPFN NHFN PVALUE HVALUE XVALUE
 3 1 2 1 21.4618E-01 1.295E6 15.87E6
*HMGA GVAL
1.6E6 1.0.9999.0001

(...)

*IBD1 IBD2 ISPC NPFN NHFN PVALUE HVALUE XVALUE
 50 1 2 1 21.4618E-01 1.294E6 15.87E6
*HMGA GVAL
.29E6 1.0.9999.0001

*IBD1 IBD2 ISPC NPFN NHFN PVALUE HVALUE XVALUE
 51 1 2 1 21.4618E-01 1.294E6 15.87E6
*HMGA GVAL
.29E6 1.0.9999.0001

*IBD1 IBD2 ISPC NPFN NHFN PVALUE HVALUE XVALUE
 52 1 2 1 21.4618E-01 1.294E6 15.87E6
*HMGA GVAL
.29E6 1.0.9999.0001

*IBD1 IBD2 ISPC NPFN NHFN PVALUE HVALUE XVALUE
 53 1 2 1 21.4618E-01 1.294E6 15.87E6
*HMGA GVAL
.29E6 1.0.9999.0001

*IBD1 IBD2 ISPC NPFN NHFN PVALUE HVALUE XVALUE
 54 1 2 1 21.4618E-01 1.294E6 15.87E6
*HMGA GVAL
.29E6 1.0.9999.0001

*IBD1 IBD2 ISPC NPFN NHFN PVALUE HVALUE XVALUE
 55 1 2 1 23.6544E-02 1.294E6 15.87E6
*HMGA GVAL
.29E6 1.0.9999.0001

*IBD1 IBD2 ISPC NPFN NHFN PVALUE HVALUE XVALUE
 1 11 1 0 0 15.8E6 2.591E6
*HMGA GVAL
1.6E6 1.0.9999.0001

*IBD1 IBD2 ISPC NPFN NHFN PVALUE HVALUE XVALUE
 2 11 1 0 0 15.8E6 2.591E6
*HMGA GVAL
1.6E6 1.0.9999.0001

*IBD1 IBD2 ISPC NPFN NHFN PVALUE HVALUE XVALUE
 3 11 1 0 0 15.8E6 2.591E6
*HMGA GVAL
1.6E6 1.0.9999.0001

*IBD1 IBD2 ISPC NPFN NHFN PVALUE HVALUE XVALUE
 4 11 1 0 0 15.8E6 2.591E6
*HMGA GVAL
1.6E6 1.0.9999.0001

*IBD1 IBD2 ISPC NPFN NHFN PVALUE HVALUE XVALUE

```

```

5 11 1 0 0 15.8E6 2.591E6
*HMGA GVAL
1.6E6 1.0.9999.0001

```

```

*IBD1 IBD2 ISPC NPFN NHFN PVALUE HVALUE XVALUE
6 11 1 0 0 15.8E6 2.591E6
*HMGA GVAL
1.6E6 1.0.9999.0001

```

(...)

```

*IBD1 IBD2 ISPC NPFN NHFN PVALUE HVALUE XVALUE
51 11 1 0 0 15.8E6 2.591E6
*HMGA GVAL
1.6E6 1.0.9999.0001

```

```

*IBD1 IBD2 ISPC NPFN NHFN PVALUE HVALUE XVALUE
52 11 1 0 0 15.8E6 2.591E6
*HMGA GVAL
1.6E6 1.0.9999.0001

```

```

*IBD1 IBD2 ISPC NPFN NHFN PVALUE HVALUE XVALUE
53 11 1 0 0 15.8E6 2.591E6
*HMGA GVAL
1.6E6 1.0.9999.0001

```

```

*IBD1 IBD2 ISPC NPFN NHFN PVALUE HVALUE XVALUE
54 11 1 0 0 15.8E6 2.591E6
*HMGA GVAL
1.6E6 1.0.9999.0001

```

```

*IBD1 IBD2 ISPC NPFN NHFN PVALUE HVALUE XVALUE
55 11 1 0 0 15.8E6 2.591E6
*HMGA GVAL
1.6E6 1.0.9999.0001

```

*

```

*****
* Group 14 - Output Options
*****

```

```

*NGRP N1 NOU1 NOU2 NOU3 NOU4 IPRP IOPT IRWR
14 5 0 0 0 0 0 2 0

```

```

*PRTC

```

```

* 12 33 45

```

```

* 14 54 80

```

```

0

```

```

0

```

```

*MXDP IGRF NLLR

```

```

300 0 0

```

```

* DTMIN DTMAX TEND RTWFP TMAX
1E-6 .001 5. 70.0 999900.

```

```

* EDINT GFINT SEDINT

```

```

1. .5 .1

```

```

* DTMIN (if negative stop)

```

```

-.001

```

Appendix F

COBRA-TF FILE: "SETUP.F"

Changes made are declared with: *cchecker*

(...)

```

850 continue
c
c set axial power profiles.
c
  if (naxp.lt.1) go to 1000
  do 925 n=1,naxp
    jone = 1
    jnodes = ndxp1
c find rod that uses table n.
  do 855 nr=1,nrrod
    if (iaxp(nr).ne.n) go to 855
    jone = jfst(nr)
    jnodes = jflend(nr)
    go to 856
855 continue
c zero table
c
856 continue
c
  do 860 j=1,ndxp1
    axialp(n,j) = 0.0
860 continue
  naxnn = naxn(n)
c convert table to feet.
  do 862 i=1,naxnn
    y(n,i)=y(n,i)/12.0
cchecker if (icobra.ne.0) y(n,i)=y(n,i)*12./3.2808
cchecker already converted to brit. units in setin.f
862 continue
c set power at bottom of rod.
  jone = jone-1
  xbot = x(jone)
  xbot1 = xbot
  xtop = xbot+0.25*(x(jone+1)-xbot)
  do 865 i=2,naxnn
    if (y(n,i).le.xbot) go to 865
    pbot = axial(n,i-1)+(axial(n,i)-axial(n,i-1))*(xbot-y(n,i-1))/
    + (y(n,i)-y(n,i-1))
    ione = i
    go to 866
865 continue
866 continue
c
  pfract = 0.0
  ifract = 0
  jx = jone
  do 890 i=ione,naxnn
    xm = y(n,i-1)
    xp = y(n,i)
870 continue
    if (xtop.gt.xp) go to 880
c find power at top of node.
    ptop = axial(n,i-1)+(axial(n,i)-axial(n,i-1))*(xtop-xm)/(xp-xm)
    if (ifract.gt.0) go to 875
c integral is equal to average of pbot and ptop.
    axialp(n,jx) = 0.5*(pbot+ptop)
    go to 885
c integral is the sum of one or more steps.
c

```

(...)

Appendix G

COUPLING RESULTS

Axial water temp. distribution in PWR fuel assembly (GRS benchmark)

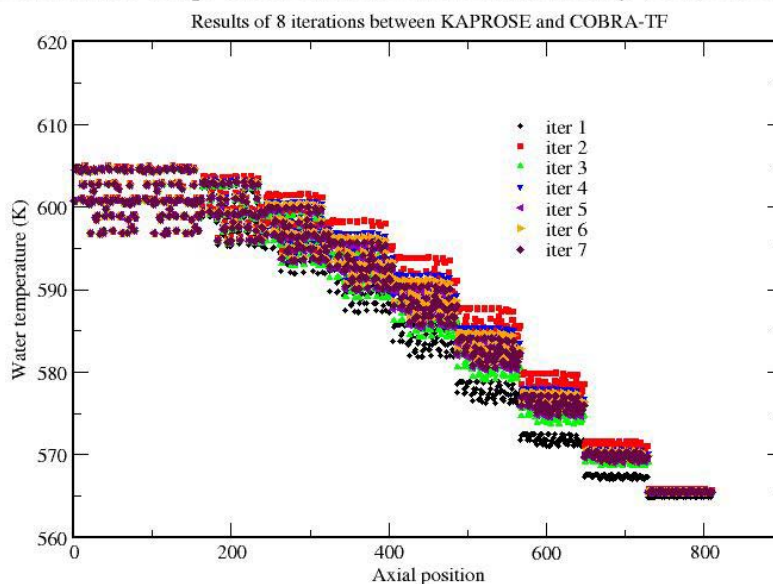


Figure G-1: Coupling - Water temperature [Ref. XI]

(Axial position – node number from top to bottom)

Axial fuel temperature distribution in PWR fuel assembly (GRS benchmark)

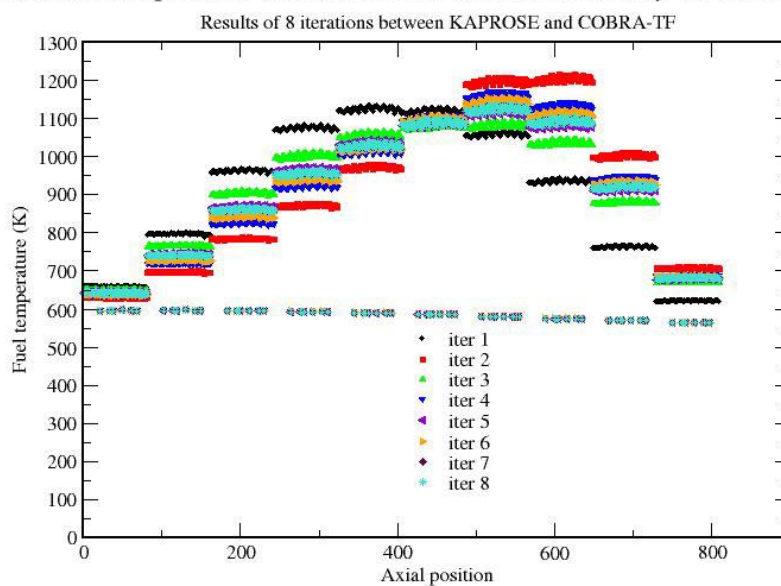


Figure G-2: Coupling - fuel temperature [Ref. XI]

(Axial position – node number from top to bottom)

Axial water density distribution in PWR fuel assembly (GRS benchmark)

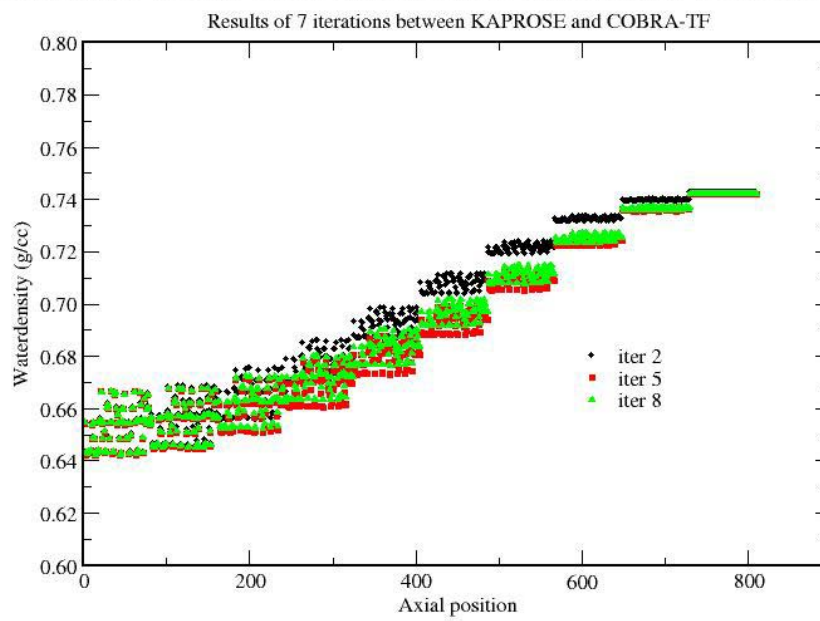


Figure G-3: Coupling - Water density [Ref. XI]
(Axial position – node number from top to bottom)

Appendix H

REFERENCES

[Ref. i] The RELAP5-3D® Code Development Team, „RELAP5-3D® CODE MANUAL, VOLUME I: CODE STRUCTURE, SYSTEM MODELS, AND SOLUTION METHODS“, INEEL-EXT-98-00834, April 2005

[Ref. ii] T. Downar, „PARCS v2.6 U.S. NRC Core Neutronics Simulator - USER MANUAL“, Purdue University (11/06/04)

[Ref. iii] X-5 Monte Carlo Team, „MCNP — A General Monte Carlo N-Particle Transport Code, Version 5“, LA-UR-03-1987, April 24, 2003

[Ref. iv] NORMA: E. Brega, R. Fontana, E. Salina, "The NORMA-FP Program to Perform a Subchannel Analysis from Converged Coarse-Mesh Nodal Solutions (Rev. 3)", ENEL-DSR-CRTN-N5/91/05/MI, Milan, September 1991

[Ref. V] Bench Mark: D.Porsch, „Spezifikation eines DWR-Brennelementes, UO₂ (4 w/o U-235) 18x18 -24, für Vergleichrechnungen“, Framatome ANP GmbH, Erlangen, July 2004

[Ref. VI] Mittag, Grundmann, Koch, Semmrich, "Erzeugung und Nutzung von Bibliotheken von Zwei-Gruppen-Diffusionsparametern zur Berechnung eines KWU-Konvoi-Reaktors mit dem Reaktordynamik-Programm DYN3D", FZR-346 (ISSN 1437-322X), April 2002

[Ref. vii] D. Basile "COBRA-EN, an Upgrade Version of COBRA-3C/MIT Code for Thermal-Hydraulic Transient Analysis of Light Water Reactor Fuel Assemblies and Cores", ENEL, ,December 1987

[Ref. viii] Analysis of FLECHT-SEAT 163-Rod Blocked Bundle Data Using COBRA-TF, NRC/EPRI/Westinghouse Report No.15

[Ref. ix] Thurgood, M.J., et al., "COBRA-TRAC: A Thermal-Hydraulic Code for Transient Analysis of Nuclear Reactor Vessels and Primary Coolant Systems," NUREG-CR-3046 (PNL-4385), Volumes 1-5, March 1982

[Ref. X] C.H.M. Broeders, "Entwicklungsarbeiten fuer die neutronenphysikalische Auslegung von Fortschrittlichen Druckwasserreaktoren (FDWR) mit kompakten Dreiecksgittern in hexagonalen Brennelementen", KFK 5072, 1992

[Ref. XI] C. Broeders, IRS, FZK, August 2005

[Ref. XII] C. Frepoli, L.E. Hochreiter; "Description of the Modifications included in the RBHT Version of COBRA-TF"; Penn State University, Mechanical and Nuclear Engineering Department; March 2000

[Ref. xiii] EPRI NP-2511-CCM, Volume 1, Revision2; RP-1584-1: Computer Code Manual July 1985; "VIPRE01: A Thermal-Hydraulic Code for Reactor Cores, Volume 1: Mathematical models"

D.L. Aumiller et al., "Incorporation of COBRA-TF in an integrated code system with RELAP5-3D using semi-implicit coupling", Bettis Atomic Power Laboratory, 2002

P.Oberle, "Erstellung einer 78-Gruppenkonstanten Bibliothek mit Energien bis 150 MeV für KAPROS", FZK, October 2004

V. Baylac-Domengetroy, "Investigations related to the generation of reaction products in the target of Accelerator Driven Systems for nuclear waste incineration", FZKA 6908, FZK, December 2003